

**CLASSIFIED DOCUMENT**

This document contains classified information relating to the National Defense of the United States within the meaning of the Espionage Act, USC 50:31 and its transmission or the revelation of its contents in any manner to an unauthorized person is prohibited by law. Information so classified may be disclosed only to persons in the military and naval Services of the United States, appropriate civilian officers and employees of the Federal Government who have a legitimate interest therein, and to United States citizens of known loyalty and discretion who of necessity must be informed thereof.

**TECHNICAL NOTES**

**NATIONAL ADVISORY COMMITTEE FOR AERONAUTICS**

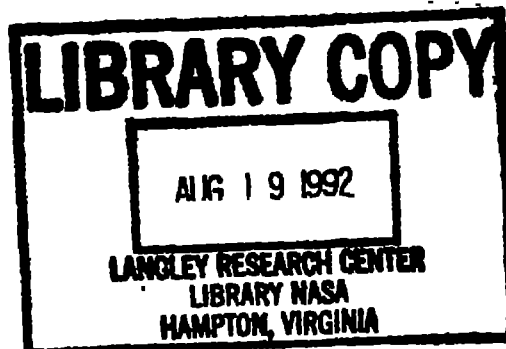
**No. 848**

**NORMAL-PRESSURE TESTS OF CIRCULAR PLATES**

**WITH CLAMPED EDGES**

**By Albert E. McPherson, Walter Ramberg, and Samuel Levy  
National Bureau of Standards**

**June 1942**



# NATIONAL ADVISORY COMMITTEE FOR AERONAUTICS

## TECHNICAL NOTE NO. 848

### NORMAL-PRESSURE TESTS OF CIRCULAR PLATES WITH CLAMPED EDGES

By Albert E. McPherson, Walter Ramberg, and Samuel Levy

#### SUMMARY

A fixture is described for making normal-pressure tests of flat plates 5 inches in diameter in which particular care was taken to obtain rigid clamping at the edges. Results are given for 19 plates, ranging in thickness from 0.015 to 0.072 inch. The center deflections and the extreme-fiber stresses at low pressures were found to agree with theoretical values; the center deflections at high pressures were 4 to 13 percent greater than the theoretical values. Empirical curves are derived of the pressure for the beginning of permanent set as a function of the dimensions of the plate and the tensile properties of the material.

#### INTRODUCTION

The normal-pressure tests of circular plates described in this report are part of a program of tests of flat plates under normal pressure that has been carried on at the National Bureau of Standards for the Bureau of Aeronautics, Navy Department, since 1927. This program was originally intended to study only rectangular plates of dimensions and materials corresponding to the plating used in the float bottoms and hull bottoms of seaplanes. The ultimate purpose of the tests was the derivation of a design formula or chart for calculating the thickness of bottom plating required to resist washboarding due to the impact pressure upon landing on and taking off from rough water.

The pressure required to produce washboarding was determined in the laboratory by normal-pressure tests of a large number of rectangular plates clamped at the edges and of several plates whose edges were free to rotate throughout the test. Results of these tests will be the subject of a subsequent paper.

A comparison of the observed deformations of the rectangular plates with the deformations derived from available theories showed both systematic and irregular differences. These differences were of sufficient magnitude to make impossible the derivation of a useful and fairly general relation for the pressure at which washboarding in such plates would become pronounced. It was not possible to determine from the work on rectangular plates alone to what degree the differences were due to a failure to satisfy the theoretical edge conditions and to what degree they were due to incompleteness of the theory itself, especially in respect to giving the stresses in the plate.

It was believed that more nearly ideal clamping conditions could be obtained for circular plates. Furthermore, it was known that the theory of circular plates with large deflections as developed by Stewart Way (reference 1) would give a rigorous basis of comparison with the measured stresses.

A careful study of the deformation of circular plates following Way's theory in the elastic region, it was felt, would lead to a better understanding of the mechanism of washboarding and might suggest a successful approach to the tests on rectangular plates.

#### SPECIMENS

The tests included seven materials as follows (see also table 1):

24S-BT alclad aluminum-alloy sheet 0.0406 to 0.0632 inch in thickness.

17S-BT aluminum-alloy sheet 0.0211 to 0.0723 inch in thickness.

17S-T aluminum alloy sheet 0.0209 to 0.0627 inch in thickness.

Low-strength aluminum-alloy sheet of unknown composition 0.015 inch in thickness.

24S-T aluminum-alloy sheet 0.0149 and 0.0184 inch in thickness.

18:8 stainless-steel sheet 0.0199 inch in thickness, and

MH magnesium-alloy sheet 0.0411 inch in thickness

All plates had the same diameter for the circular periphery along which they were clamped, that is, 5 inches. The individual plates were identified by letters A to S. (See table I.)

Tensile properties were determined on coupons cut both longitudinally and transversely out of the sheet from which the plates had been cut. Pairs of 2-inch Tuckerman optical strain gages were used to measure the strains near the center of the tensile specimens. Figures 1 to 7 show the resulting tensile stress-strain curves. The yield strengths (0.002 offset method) obtained from the stress-strain curves are given in table I. Only the magnesium alloy showed practically the same tensile properties in a longitudinal and a transverse direction. The longitudinal tensile yield strengths for the other materials were from 10 to 26 percent higher than the transverse tensile yield strengths.

## TESTS

### Loading

In the design of the fixture for subjecting circular plates to normal pressure particular care was taken to approach the ideal end conditions of rigid clamping along the periphery of the plate.

A sectional drawing of the fixture is shown in figure 8. A top view is given in figure 9. The plate specimen A (fig. 8) forms the top face of a chamber C to which oil pressure is applied through the line D; a dummy plate B of the same dimensions and of the same material as the specimen forms the bottom face of the chamber. Plates A and B are clamped between the steel rings E and G and the spacer F by forces acting through the 16 symmetrically placed clamping bars H. The symmetrical arrangement with two identical plates A and B serves to minimize rotation about the circumference of the clamping ring E by the hydrostatic load. An approximately uniform distribution of clamping forces acting on the plates was obtained, in a peripheral direction, by tightening each bolt I acting on the clamping bars an approximately equal amount and, in a radial direction, by letting the clamping bars act centrally through the crown of the clamping rings E and G. Metal shims K (figs. 8 and 10) twice as thick as the test plate were placed between the outer end of the clamping

bars and the reaction ring L to level the bars H. A series of concentric grooves 0.01 inch deep and spaced 0.05 inch were cut in the contact surfaces of the clamping rings E and G and the spacer F to prevent slipping of the plates A and B.

An over-all view of the test apparatus is given in figure 11. A hydrostatic pressure up to 600 pounds per square inch could be applied to the plate through tube D by means of the hand pump L. The pressure in the chamber O was measured from an independent pressure line M by a standpipe Y for pressures up to 1 pound per square inch, by the U-tube N for pressures from 1 to 20 pounds per square inch, by the Bourdon-tube gage V for pressures from 20 to 100 pounds per square inch, and by the Bourdon-tube gage W for pressures from 100 to 300 pounds per square inch. The error in reading pressure was estimated as less than 0.01 pound per square inch in the case of the standpipe, less than 0.1 pound per square inch in the case of the U-tube, and less than 1 pound per square inch in the Bourdon-tube gages V and W. Approximate values of pressure above 300 pounds per square inch were obtained from the Bourdon-tube gage X mounted on the hand pump.

The loading fixture was proof-tested by subjecting a pair of 0.06-inch aluminum-alloy plates to a pressure of 600 pounds per square inch. This pressure was sufficient to "dish in" the plates far beyond the elastic range; nevertheless, there was no sign of slipping at the edge and there was only a negligible amount of leakage. The pressure could be maintained with a small amount of pumping after the creep due to yielding of the plate had become small.

If slipping is neglected, the principal deviations from the conditions of an ideally clamped flat plate are probably due to one of the following effects:

A. The setting up of initial tension (or compression) in the plate during the clamping in the fixture.

B. The rotation of the clamping rings E and G (fig. 8) caused by the bending moments set up at the periphery of the plate due to the normal pressure.

C. The contraction of the diameter of the clamping rings by the nonuniform tension present in the plate under load.

D. Deviations from flatness at no load.

The effect of the first three deviations from ideal conditions on the center deflection of the plate is discussed in appendixes A, B, and C and, on the basis of those discussions, three "deviation indices" are derived for the relative deviation from ideal behavior. Deviations from flatness are discussed for the special case of initial bowing into a spherical surface in appendix D.

Effect A will cause a decrease in center deflection at low loads, ( $w_0/h < 1$ ) given approximately by equation (A7) in appendix A:

$$-\left(\frac{\Delta w_0}{w_{00A}}\right) = 1.833 (1 - \mu^2) \frac{\sigma_t a^2}{Eh^3} \quad (1a)$$

where

$$\Delta w_0 = w_0 - w_{00}$$

$w_0$  center deflection with a uniform membrane tension  $\sigma_t$  due to clamping

$w_{00}$  center deflection for ideal clamping ( $\sigma_t = 0$ )

$E$  Young's modulus of plate material

$\mu$  Poisson's ratio of plate material

$a$  radius of plate

$h$  thickness of plate

Effect A causes a decrease in center deflection of an elastic circular membrane (i.e., circular plate with large deflections before yielding) given approximately by equation (A21):

$$-\left(\frac{\Delta w_0}{w_{00A}}\right) = \frac{1 - \mu}{2} \frac{\sigma_t}{E} \frac{a^2}{w_0^2} \quad (1b)$$

that is, the effect decreases inversely with the square of the center deflection.

Effect B will cause an increase in center deflection given approximately by equation (B10)

$$\left(\frac{\Delta w_0}{w_{00B}}\right) = \frac{\lambda E h^3}{3 (1 - \mu^2) a} \quad (2)$$

where

$\lambda$  rotation of clamping ring due to unit moment per unit length of clamping edge

Effect C will cause an increase in center deflection. If the plate behaves like an elastic membrane, this increase is given approximately by equation (C14)

$$\left(\frac{\Delta w_0}{w_{00C}}\right) = \frac{1}{3} \frac{\kappa h E}{1 - \mu} \quad (3)$$

where

$\kappa$  specific contraction of diameter due to unit radial force per unit length along clamped edge

The effect D will generally cause a change in center deflection of the plate as an elastic membrane. It has no effect on the deflection due to bending which predominates in the Kirchhoff range ( $w_0/h \ll 1$ ). If the plate is initially bowed into a spherical surface with center deflection  $w_1$ , the increase in deflection as an elastic membrane ( $w_0/h \gg 1$ ) is given approximately by (D6)

$$\left(\frac{\Delta w_0}{w_{00D}}\right) = -\frac{2}{3} \frac{w_1}{w_0} = -\frac{2}{3} \frac{w_1}{h} \frac{w_0}{h} \quad (4)$$

Initial bowing into a spherical surface will have a small effect on the deflection as an elastic membrane, provided that the initial center deflection is small compared with the thickness of the plate. It is believed that this condition was satisfied by most of the plates tested. The estimated initial center deflection is given in the last column of table B. It was less than 10 percent of the plate thickness except for plates K, M, O, P, and R.

The spring constants  $\lambda$  and  $\kappa$  are characteristics of the test fixture. They were determined experimentally as described in appendixes B and C with the result

$$\lambda = 1.3 \times 10^{-7} \left(\frac{1}{lb}\right)$$

$$\kappa = 2 \times 10^{-8} \left(\frac{in.}{lb}\right)$$

Substitution of these values in (2) and (3) gave the values of  $\left(\frac{\Delta w_0}{w_{00}}\right)_B$  and  $\left(\frac{\Delta w_0}{w_{00}}\right)_0$  listed in table 3. The effect on the center deflection is less than 1 percent in every case. It may be concluded that the fixture provides a close approximation to rigid clamping.

Two methods were used for computing the relative increase in center deflection (1a) due to membrane stresses set up by the clamping procedure. In the case of plates with thickness above 0.04 inch, the deviation (1a) was computed as outlined in appendix A (discussion of equation (A22)) from the initial slope of the deflection-pressure curve and from the known value of  $\lambda$ . A different procedure was applied for plates of thickness less than 0.04 inch because accurate values of initial slope were not available. In the case of these plates, the effects B and 0 were neglected and (1a) was taken as the deviation from the theoretical deflection according to Way's theory for an ideally clamped circular plate (reference 1). The resulting deviations in the Kirchhoff range ( $w_0/h \ll 1$ ) are shown in the third column of table 8. They ranged from -48 percent to 50 percent. The deviation was less than 10 percent for only 8 of the 19 plates tested. The formula indicated an initial tension  $(\Delta w_0/w_{00})_A < 0$  in 13 plates and an initial compression  $(\Delta w_0/w_{00})_A > 0$  in 3 plates.

### Deflection

The deflection of the plates was measured relative to the "strain free" circular reference frame  $A_1$  (fig. 12) by means of a dial micrometer  $B_1$ . The helical plunger spring was removed from the dial so that the force on the plate was little more than the weight of the plunger and ball-pointed extension. The dial was mounted so that it could be located along any diameter in steps of 1/20 inch by means of the circumferentially notched bar  $H_1$  in the V-notched support  $I_1$  and indexing rings  $G_1$  and  $G_2$ . The outer ring  $G_2$  was supported on three posts  $D_1$ ,  $E_1$ ,  $F_1$  that rested on steel balls whose sockets constituted a point-line-plane support.

The smallest subdivision on the dial gage indicated 1/1000 inch. Readings on a given plate could be repeated within this value. The error in reading caused by the fact that the support points of the reference frame were



at  $D_1$ ,  $M_1$ , and  $F_1$  (figs. 8 and 12), instead of at the rim of the plate was estimated by observing the deflection of the rim with increasing pressure. A deflection of less than 1/1000 inch was observed on an 0.050-inch aluminum-alloy plate at a pressure of 300 pounds per square inch.

As the pressure increases, the shape of the deflected surface changes from that typical of a heavy clamped plate with zero slope at the edges to that characteristic of a thin skin. This transition is brought out clearly in the plot of figure 13 giving the ratio of the measured deflection to the center deflection for plate M at pressures of 2 and of 30 pounds per square inch.

In the case of most of the circular plates tested only the variation of center deflection with pressure was measured. After every second or third reading of center deflection, the pressure was reduced to a low initial value and the permanent set at the center was measured. Figures 14 to 20 show curves of total deflection and of permanent set at the center obtained in this manner for the 19 plates tested.

At low loads the center deflection was found to increase directly with the pressure; it increased more slowly as the membrane stresses became important and it approached a linear variation with pressure as yielding in the plate became pronounced. The permanent set at the center increased at an increasing rate and, except for plates O, P, Q, and R, approached a straight line that was nearly parallel to the asymptotic straight line for the total deflection at high pressures. The intersection of the first straight line with the horizontal axis defines a pressure that has been suggested by Commander R. D. MacGart as a convenient measure of yielding in the plate. This pressure is referred to as the "Navy yield pressure." The permanent set corresponding to this pressure was found to range from 0.002 to 0.009 inch. The Navy yield pressure was in no case greater than the pressure corresponding to a permanent set of 1/500 the diameter of the plate (0.01 in.). This pressure and the pressure for a set of 1/200 the diameter (0.025 in.) are also given in table 1.

#### Strain

Surface strains were measured on the 0.032-inch 17S-T aluminum-alloy plate M with 1-inch Tuckerman strain gages

placed directly on the surface of the plate (fig. 21). The strain readings were corrected for the apparent strain due to bowing of the plate between gage points by adding a term  $\frac{1}{24} \left( \frac{l}{r} \right)^2$  where  $l$  is the gage length (1 in.) and  $r$  is the average radius of curvature of the plate between gage points (obtained from the deflection curve of the plate). A derivation of this correction will be found on page 7 of reference 2.

Figure 22 shows the average radial strain over a 1-inch gage length at a point 1.5 inches from the center of the plate as a function of the pressure for a diameter in the direction of rolling and a diameter at right angles to that direction. The strain in the direction of rolling was found to be consistently smaller than that across the direction of rolling, the difference between the two reaching about 5 percent at high pressures.

The surface strains shown in figure 22 are average values over a gage length of 1 inch, that is, over a length that was 40 percent of the radius of the plate. Local values of radial strain on another 0.032-inch 17S-T aluminum-alloy plate M' were obtained within the elastic range by measuring average strains on overlapping gage lines and then applying the relations derived by Greenspan (reference 3) for determining a function from a set of measured mean values of that function.

Figure 23 shows the distribution of radial surface strain in the plate for a number of pressures within the elastic range. The curves show that, with increasing pressure, the point of inflection marking the transition from tensile to compressive strains moves toward the edge of the plate.

Strains over a 0.1-inch gage length at the center of the plate on another 0.032-inch 17S-T plate M'' were measured by a Heisse transfer (reference 4) combined with a 1-inch Tuckerman strain gage. The results are shown in figure 24.

Figures 22 and 24 both show that the strain, like the center deflection, increased at a decreasing rate as the pressure was increased up to pressures sufficient to cause considerable yielding of the material; from this point on the strain increased more rapidly.

## ANALYSIS

## Deflection

The shape of the curve into which an elastic plate is deflected by normal pressure changes continuously as the plate passes from a condition where practically all of the load is carried by bending to one where practically all of the load is carried by membrane action. The ratio  $w_0/h$  of center deflection  $w_0$  to plate thickness  $h$  can be used as a parameter to describe the change in shape of the deflection curve. If  $w_0/h \ll 1$  the deflection is that for a Kirchhoff plate with clamped edges (e.g., reference 5, p. 56):

$$\frac{w}{w_0} = \left[ 1 - \left( \frac{r}{a} \right)^2 \right]^2 \quad (5)$$

while if  $w_0/h \gg 1$  the deflection is that for a thin skin whose shape is according to Hencky (reference 6), for  $\mu = 0.3$ :

$$\frac{w}{w_0} = 1 - 0.886 \frac{r^2}{a^2} - 0.088 \frac{r^4}{a^4} - 0.020 \frac{r^6}{a^6} - 0.006 \frac{r^8}{a^8} - \dots \quad (6)$$

The deflection curves corresponding to these two extreme cases are shown in figure 13, together with experimental values for a plate without appreciable permanent set at the center and with ratios  $w_0/h = 0.72$ ,  $w_0/h = 3.12$ .

There will be a further change in the shape of the deflection curve as yielding becomes appreciable. If the yielding is localized near the edge of the plate as in a relatively thick plate ( $h/a > 0.025$ ), the shape of the deflection curve will approach that of a plate with freely supported edges (see reference 5, p. 57):

$$\frac{w}{w_0} = 1 - 1.245 \frac{r^2}{a^2} + 0.245 \frac{r^4}{a^4} \quad (7)$$

In a very thin plate the yielding will quickly spread over the entire plate, which will then tend to go into a spherical surface like a membrane under constant tension. The shape of the deflection curve is given by:

$$\frac{w}{w_0} = 1 - \frac{r^2}{a^2} \quad (8)$$

Both these curves are shown in figure 25 together with experimental deflection curves for a thick 17S-T aluminum-alloy plate ( $h/a = 0.0356$ ,  $w_0/h = 1.313$ ) and for a thin plate of the same material ( $h/a = 0.0128$ ,  $w_0/h = 5.01$ ). Most of the plates tested for the present investigation approached the condition of a membrane described by equation (8) as the pressure was increased.

The relation between center deflection and pressure for an elastic plate of medium thickness with clamped edges has been investigated by approximate methods by a number of authors. Nadai (reference 5, p. 297, equation (57)) derived the relation

$$\frac{w_0}{h} + 0.583 \left(\frac{w_0}{h}\right)^3 = \frac{3}{16} \frac{p}{E} \left(\frac{a}{h}\right)^4 (1 - \mu^2) \quad (9)$$

by solving the differential equation for a plate with large deflection subjected to a nearly uniform pressure distribution. Timoshenko (reference 7, p. 319, equation (219)) derived

$$\frac{w_0}{h} + 0.488 \left(\frac{w_0}{h}\right)^3 = \frac{3}{16} \frac{p}{E} \left(\frac{a}{h}\right)^4 (1 - \mu^2) \quad (10)$$

on the basis of an assumed radial displacement combined with energy considerations. Federhofer (reference 8) derived

$$\frac{w_0}{h} + \frac{(19 - 9\mu)(1 + \mu)}{40} \left(\frac{w_0}{h}\right)^3 = \frac{3}{16} \frac{p}{E} \left(\frac{a}{h}\right)^4 (1 - \mu^2) \quad (11)$$

from the differential equation of the problem together with a suitable assumption for the radial distribution of membrane tension. For  $\mu = 0.3$  the coefficient of  $(w_0/h)$  becomes 0.529, which is between the corresponding values of equations (9) and (10). A procedure analogous to Föppl's solution (reference 9, p. 230) for the center deflection of a rectangular plate (appendix E) gives

$$\frac{w_0}{h} + 0.588 \left(\frac{w_0}{h}\right)^3 = \frac{3}{16} \frac{p}{E} \left(\frac{a}{h}\right)^4 (1 - \mu^2) \quad (12)$$

Boobnov (reference 10) solved the differential equation

of a circular plate of medium thickness with clamped edges upon the assumption that the membrane tension is constant throughout the plate. An "exact" solution of the differential equation for a circular plate with clamped edges was first obtained by Stewart Way (reference 1). Way's solution as well as the approximate solutions (9) to (12) and Boobnov's solution are shown graphically in figure 26 for the special case  $\mu = 0.3$ . The six curves differ from each other less than 6 percent. Observed values of center deflection are shown as open points for pressures at which the permanent set was less than  $1/500$  the diameter of the plate and as solid points for greater pressures.

It is seen that the experimental deflections consistently exceed the theoretical values by 4 to 12 percent for  $pa^4/Eh^4 > 15$ . At low pressures the theoretical curves and the experimental points are in agreement.

### Stresses

The stresses in a circular plate with clamped edges under normal pressure have been evaluated from the theory by Way (reference 1) for center deflections up to 1.2 times the thickness of the plate. An extension to greater values of  $w_0/h$  seemed desirable since some of the plates tested at the National Bureau of Standards (e.g., plate K) were still nearly elastic, that is, showed negligible permanent set, at  $w_0/h = 4$ . It was decided, accordingly, to extend Way's solution, but this extension was not carried beyond  $w_0/h = 1.5$  because of the excessive amount of computation involved.

It appeared necessary to resort to one of the approximate theories cited in references 5, 7, 8, 9, and 10 in order to estimate the stresses for  $w_0/h > 1.5$ . Examination of these approximate theories showed that only Nadai's approximate theory gave stresses in close agreement with the values given by Way's theory. This result was to be expected since Nadai's theory is the only one of the approximate theories that gives a solution of the differential equation for a plate with large deflections. It differs from Way's solution only in assuming a convenient but not quite uniform pressure distribution while Way solved for a strictly uniform pressure.

The calculations by Nadai's theory were accordingly

extended to values of  $w_0/h = 4$ . (At  $w_0/h = 4$  the assumed pressure deviated from its average value about 25 percent at the center and about 5 percent at the edge.) The resulting pressure deflection curve is shown as curve F in figure 26. It agrees with those given by equations (9) and (12). The extreme-fiber bending stresses and the median-fiber tensile stresses in a radial direction for the center of the plate and the edge of the plate are plotted against the center deflection in figure 27. It is evident from figure 27 that Nadai's and Way's theories are in good agreement.

The plate with large deflection just as the Kirchhoff plate is most highly stressed along the clamped edge, the maximum radial stress being about three times as large as the maximum stress at the center for  $w_0/h = 4$ . The median-fiber tension at the center exceeds the extreme-fiber bending stress for  $w_0/h > 2$ . At the edge the extreme-fiber bending stress is more than five times as large as the median-fiber tension even for  $w_0/h = 4$ .

Radial strains  $\epsilon_r$  calculated from the stresses according to Way's theory and according to Nadai's theory (fig. 27) by substitution in

$$\epsilon_r = \frac{1}{E} (\sigma_r - \mu \sigma_t)$$

where  $\sigma_r$  is the radial stress and  $\sigma_\phi$  the tangential stress, are compared with measured strains for plates M', M'', in figures 23 and 24. The theoretical strains exceeded the observed strains for plate M' and they were less than the observed strains for plate M''. The differences may be due to differences in clamping conditions. Curves of center deflection against pressure from which such differences could be estimated were not obtained for these two plates because the strain gages interfered with measurement of the center deflection.

#### Permanent Set

Theoretical values for the pressure at which permanent set at the center became noticeable were derived as follows: It was assumed that the beginning of permanent set would be associated with yielding either along the edge of the plate or at the center of the plate and that this yielding could be computed from the theoretical stresses upon the assump-

tion of the von Mises-Hencky theory of plastic failure. According to this theory (reference 11, p. 73) plastic action will begin under the action of principal stresses  $\sigma_1$ ,  $\sigma_2$ ,  $\sigma_3$  when

$$(\sigma_1 - \sigma_2)^2 + (\sigma_2 - \sigma_3)^2 + (\sigma_3 - \sigma_1)^2 = 2\sigma_y^2 \quad (13)$$

where  $\sigma_y$  is the stress at which plastic action begins in simple tension.

At the edge of the plate

$$\sigma_1 = \sigma_{re}, \quad \sigma_2 = \sigma_{\phi e} = \mu\sigma_{re}, \quad \sigma_3 = 0 \quad (14)$$

where

$\sigma_{re}$  extreme-fiber stress in radial direction at edge of plate on concave side

$\sigma_{\phi e}$  extreme-fiber stress in tangential direction at edge of plate on concave side

The value of  $\sigma_{\phi e}$  must be equal to  $\mu\sigma_{re}$  since the tangential strain  $(\sigma_{\phi e} - \mu\sigma_{re})/E$  is assumed to be zero for perfect clamping. Substitution of equation (14) in equation (13) gives with  $\mu = 0.3$

$$\sigma_{re} = \frac{\sigma_y}{\sqrt{1 - \mu + \mu^2}} = 1.12 \sigma_y \quad (15)$$

It follows that

$$\frac{\sigma_y}{E} \frac{a^2}{h^2} = 0.89 \frac{\sigma_{re}}{E} \frac{a^2}{h^2} \quad (16)$$

According to figure 27,  $\frac{\sigma_{re}}{E} \frac{a^2}{h^2}$  is a function of the center deflection ratio  $w_0/h$  and hence, according to figure 26, a function of the pressure ratio  $\frac{p}{E} \frac{a^4}{h^4}$ . The resulting relation between  $\frac{\sigma_y}{E} \frac{a^2}{h^2}$  and  $\frac{pa^4}{Eh^4}$  is plotted as curve A to log-log scales in figures 28, 29, and 30.

The theoretical pressure for yielding at the center

may be computed in an analogous manner. The principal stresses in the plane of the plate are equal at the center so that equation (14) should be replaced by

$$\sigma_1 = \sigma_{r0}, \quad \sigma_2 = \sigma_{r0}, \quad \sigma_3 = 0 \quad (17)$$

where  $\sigma_{r0}$  is the extreme-fiber stress in a radial direction at the center of the plate, on the convex side. Substituting of equation (17) in (13) gives, in place of equations (15) and (16)

$$\begin{aligned} \sigma_{r0} &= \sigma_y \\ \frac{\sigma_y}{E} \frac{a^2}{h^2} &= \frac{\sigma_{r0}}{E} \frac{a^2}{h^2} \end{aligned} \quad (18)$$

The corresponding relation between  $\frac{\sigma_y}{E} \frac{a^2}{h^2}$  and  $\frac{pa^4}{Eh^4}$  is shown as curve B in figures 28, 29, and 30.

A comparison with the experimental yield pressures given in table 1 was made as follows: The stress  $\sigma_y$ , that is, the stress at which plastic action begins in tension, was replaced by the average of the conventional tensile yield strength in a longitudinal direction and in a transverse direction (table 1). The pressure for the beginning of plastic action was replaced by the Navy yield pressure in figure 28, by the pressure for a set at the center of 1/500 the diameter in figure 29, and by the pressure for a set at the center of 1/200 the diameter in figure 30.

The observed points for the eight 17S-RT plates fall closely on a single straight line. If the observed points for the other plates tested are also included, they may all be represented approximately by a straight line O that lies between the theoretical curves for yielding at the edge (curve A) and yielding at the center (curve B). Examination of figures 28 to 30 shows that for values of  $\sigma_y a^2 / Eh^2$  up to 80 the line O gives the measured Navy yield pressures within  $\pm 43$  percent, the pressure for a set at the center of 2a/500 within  $\pm 34$  percent, and the pressure for a set at the center of 2a/200 within  $\pm 42$  percent.

A larger scatter was found for the very thin plates



$(\sigma_{ya}^2/Eh^2 > 80)$  in which the initial tension due to clamping and the deviation from perfect flatness are likely to be largest. A large scatter is to be expected because of the use of the tensile yield strength as the parameter characterizing the beginning of plastic action of the material in the plate. This result leads to a particularly large error in the case of the alclad material, in which yielding on the surface of the plate may take place at relatively low pressure, although the "average" yield strength as determined by the tensile test may be relatively high. This view is supported by a comparison of tensile yield strengths and pressures for yielding (table 1) for the 24S-RT alclad plates and the 17S-RT aluminum-alloy plates. The tensile yield strengths of the 17S-RT material are about 9 percent lower than those of the 24S-RT alclad material and yet the 17S-RT plates have yield pressures that exceed those for the 24S-RT alclad plates by amounts up to 22 percent.

Another description of the experimental data in figures 28 to 30 was obtained by making use of the experimental result (figs. 31 to 33) that the yielding began when the center deflection of the plate reached a value which was roughly independent of the thickness and of the material of the plate. This value was about 0.11 inch for the Navy yield pressure (fig. 31), about 0.12 inch for the pressure corresponding to a set of 1/500 the diameter (fig. 32), and about 0.14 inch for a set of 1/200 the diameter (fig. 33).

The foregoing experimental result may be mathematically expressed by saying that yielding began when the ratio

$$\frac{w_0}{a} = \text{const} \quad (19)$$

Examination of figure 27 indicated that a relation of this type should hold approximately at large center deflections both if the yielding is assumed to begin when the median-fiber strain at the center reaches a critical value and when the extreme-fiber bending strain at the edge reaches a critical value.

A relation between yielding pressure and plate thickness may be obtained by inserting equation (19) in the relation between pressure and center deflection. This center-deflection relation is, according to equations (9) to (12), of the general type

$$\frac{p}{E} = k_1 \left(\frac{h}{a}\right)^4 \left[ \frac{w_0}{h} + k_2 \left(\frac{w_0}{h}\right)^3 \right] \quad (20)$$

where  $k_1$  and  $k_2$  are constants. Elimination of  $w_0$  from (19) and (20) gives the desired relation:

$$\frac{p}{E} = k_3 \left(\frac{h}{a}\right) + k_4 \left(\frac{h}{a}\right)^3 \quad (21)$$

where  $k_3$  and  $k_4$  are again constants. A determination of these constants by least squares to give the best fit to the observed values of  $p/E$  gave:

For Navy yield pressure

$$10^6 \frac{p}{E} = 1.93 \left(100 \frac{h}{a}\right) + 0.274 \left(100 \frac{h}{a}\right)^3 \quad (22)$$

For pressure at  $\text{set} = 2a/500$

$$10^6 \frac{p}{E} = 2.78 \left(100 \frac{h}{a}\right) + 0.226 \left(100 \frac{h}{a}\right)^3 \quad (23)$$

For pressure at  $\text{set} = 2a/200$

$$10^6 \frac{p}{E} = 4.45 \left(100 \frac{h}{a}\right) + 0.190 \left(100 \frac{h}{a}\right)^3 \quad (24)$$

Equations (22) to (24) are shown together with the observed points in figures 34 to 36. The scatter is of the same order as that for the more rational curves given in figures 28 to 30.

The principal difference between straight lines 0 in figures 28 to 30 and the empirical relations (22) to (24) is that the empirical relations do not involve the yield strength of the material. Their applicability to the present series of plates is explained by the fact that the strain defined by  $\sigma_{\text{yield}}/E$  is roughly constant, about 0.005, for the materials investigated (table 1). If the points for plates 0 and 8, which had values of  $\sigma_{\text{yield}}/E$  of about 0.004, are omitted, the scatter is reduced. It is safer to use the straight lines 0 (figs. 28 to 30) in the cases where  $\sigma_{\text{yield}}/E$  differs greatly from 0.005.

The points for plates H, M, O, P, Q, and R that had deviation indices greater than 20 percent according to table 2 are labeled in figures 28 to 36 for comparison with the points for the rest of the plates. It will be noticed that the scatter of points about a common curve would have been reduced by leaving these points out of consideration.

National Bureau of Standards,  
Washington, D. C., October 10, 1941.

#### APPENDIX A

##### DEVIATIONS FROM IDEAL CLAMPING DUE TO INITIAL TENSION (OR COMPRESSION) IN PLATE

The plate may be in a state of initial tension or compression due to the clamping procedure or due to differential expansion as the result of temperature changes.

Initial tension will lower the deflection of the plate in the Kirchhoff range, that is, at sufficiently low loads to make  $w_0/h \gg 1$ , by an amount that may be estimated from Nadai's analysis of a plate under normal pressure  $p$  and under a uniform compression of  $n$  units of force per unit length of circumference. The deflection at a point a distance  $r$  from the center of such a plate is, according to Nadai (reference 5, p. 255):

$$w = \frac{pa^2}{4\alpha^2 N} \left\{ \frac{2 [J_0(\alpha r) - J_0(\alpha a)]}{\alpha a J_1(\alpha a)} - 1 + \frac{r^2}{a^2} \right\} \quad (A1)$$

where

$p$  normal pressure

$\alpha^2$   $n/M$

$N$  flexural rigidity of plate  $[Eh^3/12(1 - \mu^2)]$

$E$  Young's modulus of plate material

$\mu$  Poisson's ratio of plate material

$h$  thickness of plate

and  $J_0$  and  $J_1$  are Bessel functions of the first kind given by the series expansions:

$$J_0(x) = 1 - \frac{1}{1!^2} \left(\frac{x}{2}\right)^2 + \frac{1}{2!^2} \left(\frac{x}{2}\right)^4 - \frac{1}{3!^2} \left(\frac{x}{2}\right)^6 + \dots \quad (A2)$$

$$J_1(x) = \frac{x}{2} \left[ 1 - \frac{1}{1 \times 2} \left(\frac{x}{2}\right)^2 + \frac{1}{1 \times 2 \times 2 \times 3} \left(\frac{x}{2}\right)^4 + \dots \right] \quad (A3)$$

Substituting

$$\alpha^2 = - \frac{n_t}{N} = - \frac{\sigma_t h}{N} \quad (A4)$$

where  $\sigma_t$  is the initial membrane stress, in (A1) and carrying out the series expansions (A2) and (A3) leads to the following approximate expression for the deflection in the Kirchhoff region:

$$w = \frac{pa^4}{64N} \left[ \left(1 - \frac{r^2}{a^2}\right)^2 - \frac{n_t a^2}{72N} \left(11 - 12 \frac{r^2}{a^2} + 9 \frac{r^4}{a^4} - 8 \frac{r^6}{a^6}\right) \right] \quad (A5)$$

The center deflection is

$$w_0 = w(0) = \frac{pa^4}{64N} \left(1 - \frac{11}{72} \frac{n_t a^2}{N}\right) \quad (A6)$$

If  $w_{00}$  denotes the center deflection in the ideally clamped plate ( $n_t = 0$ ) the relative increase in center deflection due to initial tension is given by

$$\left(\frac{\Delta w_0}{w_{00}}\right)_A = \frac{w_0 - w_{00}}{w_{00}} = - \frac{11}{72} \frac{n_t a^2}{N} = - 1.833 (1 - \mu^2) \frac{\sigma_t a^2}{Nh^2} \quad (A7)$$

The relative increase in radial bending moment at the edge of the plate due to the tension  $n_t$  may be calculated from (A5) as follows: The radial bending moment at any point in the plate is (reference 5, p. 57):

$$m_r(r) = - N \left( \frac{d^2 w}{dr^2} + \frac{\mu}{r} \frac{dw}{dr} \right) \quad (A8)$$

Substituting (A5) in this equation gives:

$$m_r(r) = -\frac{pa^2}{64} \left\{ -4(1+\mu) + 4(3+\mu) \frac{r^2}{a^2} - \frac{n_t a^2}{18N} \left[ -6(1+\mu) + 9(3+\mu) \frac{r^2}{a^2} - 12(5+\mu) \frac{r^4}{a^4} \right] \right\} \quad (A9)$$

The radial bending moment at the edge is

$$m_a = m_r(a) = -\frac{pa^2}{8} \left[ 1 + \frac{1}{48} (13 + 3\mu) \frac{n_t a^2}{N} \right] \quad (A10)$$

and the relative increase in radial bending moment over the bending moment  $m_{a0}$  for an ideally clamped plate ( $n_t = 0$ ) becomes:

$$\left( \frac{\Delta m_a}{m_{a0}} \right) = \frac{m_a}{m_{a0}} - 1 = \frac{1}{48} (13 + 3\mu) \frac{n_t a^2}{N} \quad (A11)$$

The effect of the initial tension  $\sigma_t$  in decreasing the center deflection at high pressure for which the plate approaches the condition of a circular membrane is given approximately by substituting  $\sigma_t$  in (04):

$$w_0 = \frac{pa^2}{4h\sigma} \quad (A12)$$

where

$$\sigma = \sigma_w + \sigma_t \quad (A13)$$

is the membrane stress in the plate at the deflection considered, consisting of the membrane stress  $\sigma_w$  due to the deflection  $w_0$  at the center, and the initial tension  $\sigma_t$ . The relative increase in center deflection over a membrane with zero initial tension is then given by

$$\frac{\Delta w_0}{w_{00}} = \frac{\sigma_0 - \sigma}{\sigma} = \frac{\sigma_0 - (\sigma_w + \sigma_t)}{\sigma_w + \sigma_t} \quad (A14)$$

An approximate value for the membrane tension  $\sigma_w$  is obtained by considering the membrane to deflect into a spherical surface. This surface coincides, for ratios  $w_0/a \ll 1$ , with the parabolic surface

$$w = w_0 \left( 1 - \frac{r^2}{a^2} \right) \quad (A15)$$

The bowing will set up an average tensile strain

$$\begin{aligned} \epsilon_w &= \frac{1}{a} \int_{r=0}^a (ds - dr) = \frac{1}{a} \int_{r=0}^a (\sqrt{dw^2 + dr^2} - dr) \\ &= \frac{1}{2a} \int_0^a \left( \frac{dw}{dr} \right)^2 dr = \frac{2}{3} \frac{w_0^2}{a^2} \end{aligned} \quad (A16)$$

This strain corresponds to an average tensile stress

$$\sigma_w = \frac{2}{3} \frac{E}{1 - \mu} \frac{w_0^2}{a^2} \quad (A17)$$

In particular

$$\sigma_0 = \frac{2}{3} \frac{E}{1 - \mu} \frac{w_{00}^2}{a^2} \quad (A18)$$

so that

$$\sigma_w = \sigma_0 \left( \frac{w_0}{w_{00}} \right)^2 = \sigma_0 \left[ 1 + \frac{\Delta w_0}{w_{00}} \right]^2 \quad (A19)$$

Substitution of this expression in equation (A14), assuming that  $(\Delta w_0/w_{00})^2 \ll 1$ , gives an equation that may be solved for  $\Delta w_0/w_{00}$  with the following result:

$$\frac{\Delta w_0}{w_{00}} = - \frac{\sigma_t}{3\sigma_0 + \sigma_t} \quad (A20)$$

Substitution of (A18) in (A20) gives:

$$\frac{\Delta w_0}{w_{00}} = - \frac{1}{1 + \frac{2}{1 - \mu} \frac{E}{\sigma_t} \frac{w_0^2}{a^2}} \approx - \frac{1}{2} (1 - \mu) \frac{\sigma_t}{E} \frac{a^2}{w_0^2} \quad (A21)$$

The relative effect of the initial tension on the center

deflection decreases with the inverse square of the center deflection.

An estimate of  $n_t = \sigma_t h$  was obtained from the observed initial slope  $w_0/p$  of the curve of center deflection against pressure upon the assumption that this slope would be equal to that for an ideally clamped plate except for the correction due to rotation of the clamping edges and due to the initial tension. The initial tension per unit length  $n_t$  is then from (B16):

$$n_t = \frac{72}{11} \left( 1 + \frac{4\lambda N}{a} - \frac{64N}{a^4} \frac{w_0}{p} \frac{N}{a^2} \right) \quad (A22)$$

where  $w_0/p$  denotes the measured initial slope of the curve of center deflection against pressure.

The values of  $n_t$  derived from (A22) were substituted in (A7) to give the deviation indices  $(\Delta w_0/w_{00})_A$  that are listed in table B.

## APPENDIX B

### DEVIATIONS FROM IDEAL CLAMPING DUE TO ROTATION OF CLAMPING RING

Rotation of the clamping rings  $E$  will have the greatest percentage effect on the deformation of the plate at low loads for which the Kirchhoff theory holds. The effect becomes negligible as the plate approaches the condition of a membrane at high pressures.

The deflection  $w(r)$  of a circular plate clamped in torsionally elastic edges may be considered as the resultant:

$$w = w_1 + w_2 \quad (B1)$$

of the deflection  $w_1$  of a plate with rigidly clamped edges (reference 5, pp. 56-57):

$$w_1(r) = \frac{p_1}{64N} (a^2 - r^2)^2 \quad (B2)$$

and of a plate with simply supported edges:

$$w_2(r) = \frac{p_2}{64N(1+\mu)} \left[ (5+\mu) a^4 - 2(3+\mu) a^2 r^2 + (1+\mu) r^4 \right] \quad (B3)$$

where

$p_1$  partial pressure required to produce deflection  $w_1$

$p_2$  partial pressure required to produce deflection  $w_2$

$p$  total pressure ( $p_1 + p_2$ )

The pressure  $p_1$  will produce a radial bending moment  $m_a$  per unit length of clamping edge:

$$m_a = m_r(a) = - \frac{p_1 a^3}{8} \quad (B4)$$

which will cause a rotation of the clamping ring:

$$\lambda m_a = - \frac{\lambda p_1 a^3}{8} \quad (B5)$$

where

$\lambda$  rotation of clamping ring (radians) due to unit moment per unit length of clamping edge

The rotation of the clamping ring (B5) must be equal to the slope of the plate at the clamping edge, which is from (B1) and (B3):

$$w'(a) = w'_1(a) + w'_2(a) = w'_2(a) = - \frac{1}{8} \frac{p_2 a^3}{(1+\mu)N} \quad (B6)$$

where primes denote differentiation with respect to  $r$ .

Setting this expression equal to (B5) gives:

$$\frac{p_2}{p_1} = \frac{(1+\mu) \lambda N}{a} \quad (B7)$$

The center deflection becomes with (B2) and (B3)

$$w_0 = w(0) = w_1(0) \left[ 1 + \frac{(5+\mu) \lambda N}{a} \right] \quad (B8)$$



The center deflection  $w_{00}$  for rigid clamping follows from (B8) with  $\lambda = 0$ . The relative increase in center deflection for a given total pressure  $p = p_1 + p_2$  is, therefore:

$$\left(\frac{\Delta w_0}{w_{00}}\right)_B = \frac{w_0}{w_{00}} - 1 = \frac{\frac{4\lambda N}{a}}{1 + (1+\mu) \frac{\lambda N}{a}} \quad (B9)$$

for sufficiently small values of  $\lambda$  ( $\frac{\lambda N}{a} \ll 1$ ), this expression is approximately:

$$\left(\frac{\Delta w_0}{w_{00}}\right)_B \approx \frac{4\lambda N}{a} = \frac{\lambda N h^3}{3(1-\mu^2)a} \quad (B10)$$

The bending moment at the edge is from (B4) and (B7)

$$\begin{aligned} m_a &= -\frac{p_1 a^3}{8} = -\frac{p a^3}{8} \left(1 - \frac{p_2}{p_1 + p_2}\right) \\ &= -\frac{p a^3}{8} \left[1 - \frac{(1+\mu) \lambda N/a}{1 + (1+\mu) \lambda N/a}\right] \end{aligned} \quad (B11)$$

and the relative increase in bending moment over the moment  $m_{a0}$  for rigid clamping ( $\lambda = 0$ ) is:

$$\left(\frac{\Delta m_a}{m_{a0}}\right)_B = -\frac{(1+\mu) \lambda N/a}{1 + (1+\mu) \lambda N/a} \quad (B12)$$

or for  $\lambda N/a \ll 1$ :

$$\left(\frac{\Delta m_a}{m_{a0}}\right)_B = -(1+\mu) \frac{\lambda N}{a} \quad (B13)$$

The spring constant  $\lambda$  was determined experimentally as follows. A pair of relatively thick aluminum-alloy plates ( $h = 0.0627$  in.) were clamped in the test fixture. A set of small prisms ( $N$ , fig. 10) were then fastened to the clamping ring to measure the rotation of the clamping ring out of a horizontal plane, by means of a Tuckerman autocollimator. Normal pressure was applied to the plate and both the rotation  $w'_a$  of the prisms and the center deflection  $w_0$  of the plate were measured at a number of

pressures  $p$ . The resulting values were found to increase linearly with the pressure so that a straight line could be drawn through the points. The slopes  $w_o/p$  and  $w'_a/p$  of these two straight lines were used to determine  $\lambda$  as follows:

If it is assumed that the plate behaves like a rigidly clamped Kirchhoff plate except for a uniform initial tension  $n_t$  and a rotation of the end clamps, the slope of the curve of center deflection against pressure curve is given by

$$\frac{w_o}{p} = \frac{w_{oo} + (\Delta w_o)_A + (\Delta w_o)_B}{p} = \frac{w_{oo}}{p} \left[ 1 + \left( \frac{\Delta w_o}{w_{oo}} \right)_A + \left( \frac{\Delta w_o}{w_{oo}} \right)_B \right] \quad (B14)$$

where  $(\Delta w_o/w_{oo})_A$  denotes the deviation for initial tension (A7) and  $(\Delta w_o/w_{oo})_B$  the deviation for rotation of the clamping rings (B10). Substituting these deviations together with the center deflection for the clamped plate (see B2)

$$w_{oo} = \frac{pa^4}{64N} \quad (B15)$$

gives

$$\frac{w_o}{p} = \frac{a^4}{64N} \left[ 1 - \frac{11}{72} \frac{n_t a^2}{N} + \frac{4\lambda N}{a} \right] \quad (B16)$$

for the initial slope of the curve of center deflection against pressure. The initial slope of the curve for rotation of the clamping rings against pressure is given by

$$\frac{w'_a}{p} = \frac{w'_a(a)}{p} = \frac{\lambda m_a}{p} \quad (B17)$$

where  $m_a$  is the radial bending moment at the edge of the plate. This expression may be written in analogy to equation (B14) as

$$\frac{m_a}{p} = \frac{m_{ao}}{p} \left[ 1 + \left( \frac{\Delta m_a}{m_{ao}} \right)_A + \left( \frac{\Delta m_a}{m_{ao}} \right)_B \right] \quad (B18)$$

where  $(\Delta m_a/m_{ao})_A$  is the relative increase in edge bending moment due to initial tension given by equation (A11), and

$(m_a/m_{ao})_p$  is the relative increase due to rotation of the edges given by equation (B12). Substituting these values in (B18) gives:

$$\frac{w'_a}{p} = \frac{\lambda m_a}{p} = -\frac{\lambda a^2}{8} \left[ 1 + \frac{1}{48} (13 + 3\mu) \frac{n_t a^2}{M} - (1 + \mu) \frac{\lambda M}{a} \right] \quad (B19)$$

Elimination of  $n_t$  from equations (B16) and (B19) gives the following equation for  $\lambda$ :

$$\frac{w'_a}{p} = -\frac{\lambda a^2}{8} \left[ 1 + \frac{3}{22} (13 + 3\mu) \left( 1 - \frac{64 M w_0}{a^4 p} \right) + \frac{67 + 7\mu}{11} \frac{\lambda M}{a} \right] \quad (B20)$$

Measurements for plate 0 gave

$$\frac{w_0}{p} = 0.00250 \text{ cu in./lb} \quad \text{and} \quad \frac{w'_a}{p} = -10^{-7} \text{ sq in./lb}$$

Substitution of these values, together with the constants -  $a = 2.5$  inches;  $h = 0.0627$  inch;  $M = 10.5 \times 10^6$  pounds per square inch; and  $\mu = 1/3$  - in equation (B20) and solving for  $\lambda$  gave

$$\lambda = 1.3 \times 10^{-7} \text{ (lb}^{-1}\text{)}$$

## APPENDIX C

### DEVIATION FROM IDEAL CLAMPING DUE TO RADIAL

#### CONTRACTION OF CLAMPING RING

The clamping ring will contract under the action of the membrane tension set up in the plate at high pressures, and this contraction will reduce the tension in the plate and will increase the center deflection corresponding to a given pressure.

An approximate estimate of this effect was obtained by replacing the plate by a membrane under uniform tension, which bulges into a spherical surface with center deflection  $w_0$ . The deflection of the membrane at a distance  $r$  from the center is then

$$w = w_0 \left( 1 - \frac{r^2}{a^2} \right) \quad (C1)$$

The curvature of the membrane is

$$\frac{1}{R} = \frac{d^2 w}{dr^2} = - \frac{2w_0}{a^2} \quad (02)$$

For equilibrium between the uniform tensile stress  $\sigma$  in the plate and the external pressure  $p$  (reference 12, p. 511):

$$\sigma = \frac{pR}{2h} = \frac{pa^2}{4w_0 h} \quad (03)$$

so that the center deflection is given by

$$w_0 = \frac{pa^2}{4h\sigma} \quad (04)$$

The membrane stress will cause an elastic contraction of the clamping ring given by

$$a_0 - a = a_0 \kappa \sigma h \quad (05)$$

where  $\kappa$  is the specific contraction along the diameter of the membrane due to unit radial tension per unit length of clamping edge.

The center deflection  $w_{00}$  for an ideally clamped plate of thickness  $h$  and of radius  $a_0$  subjected to pressure  $p$  is, according to equation (04),

$$w_{00} = \frac{pa_0^2}{4h\sigma_0} \quad (06)$$

The correction in center deflection is, therefore,

$$\frac{\Delta w_0}{w_{00}} = \frac{w_0}{w_{00}} - 1 = \left( \frac{a}{a_0} \right)^2 \left( \frac{\sigma_0}{\sigma} \right) - 1 \quad (07)$$

The membrane stress  $\sigma$  is related to the membrane strain by

$$\sigma = \frac{E}{1 - \mu} \epsilon \quad (08)$$

The value of  $\epsilon$  is given by correcting equation (A16) for the change in strain  $\kappa h \sigma$  due to contraction of the clamping ring:

$$\epsilon = \frac{2}{3} \left( \frac{w_0}{a} \right)^2 - \kappa h \sigma \quad (09)$$

Substituting (09) in (08) and solving for  $\sigma$  gives

$$\sigma = \frac{1}{\kappa h + \frac{1-\mu}{E}} \frac{2}{3} \left( \frac{w_0}{a} \right)^2 \quad (010)$$

The stress  $\sigma_0$  for a rigidly clamped plate is derived from (010) by making  $\kappa = 0$ . It follows that

$$\frac{\sigma_0}{\sigma} = \left( 1 + \frac{E}{1-\mu} \kappa h \right) \left( \frac{w_{00}}{w_0} \right)^2 \left( \frac{a}{a_0} \right)^2 \quad (011)$$

The ratio  $a/a_0$  is, from (05)

$$a/a_0 = 1 - \kappa h \sigma \quad (012)$$

Substituting (011) and (012) in (07), expanding, and neglecting terms that are small of higher order gives

$$\frac{\Delta w_0}{w_{00}} = \frac{E}{1-\mu} \kappa h - 2 \frac{\Delta w_0}{w_{00}} - 4 \kappa h \sigma \quad (013)$$

The last term on the right is negligible compared with the first term since  $\sigma \ll E$  so that, in first approximation

$$\frac{\Delta w_0}{w_{00}} = \frac{1}{3} \frac{E \kappa h}{1-\mu} \quad (014)$$

An experimental estimate of  $\kappa$  was obtained as follows: A pair of relatively thin plates ( $h = 0.0209$  in.) was clamped in the fixture. The center deflection  $w_0$  of the plate was then measured as a function of the normal pressure in a range where the plate approximated a taut membrane ( $w_0 > 10h$ , permanent set at center greater than  $4h$ ). The values of  $w_0$  thus obtained were substituted in (04) to estimate the membrane stress  $\sigma$ . The contraction in diameter,  $2a_0 - 2a$  of the clamping ring due to this membrane stress was measured by a Tuckerman strain gage (T, fig. 10) with a 5-inch gage length. Substitution of the measured values of  $a_0 - a$  and of  $\sigma$  in (05) gave six values of  $\kappa$  ranging from  $1.9 \times 10^{-8}$  to

$2.2 \times 10^{-8}$  in./lb. An average value  $\kappa = 2 \times 10^{-8}$  in./lb, was substituted in (D14) to obtain the deviation indices  $(\Delta w_0/w_{00})_0$  given in table 2.

#### APPENDIX D

##### EFFECT OF INITIAL BOWING ON CENTER DEFLECTION OF CIRCULAR MEMBRANE

Let it be assumed that a membrane of radius  $a$  is bowed into a spherical surface with center deflection  $w_1$  at no load. The increase  $w_0$  in center deflection due to a normal pressure  $p$  is then approximately, according to equation (A12),

$$w_0 = \frac{pa^2}{4h\sigma} \quad (D1)$$

where  $\sigma$  is the tensile stress corresponding to the strain  $\epsilon$  required to produce the center deflection  $w_0$ . According to equation (A16)

$$\epsilon = \frac{2}{3} \left[ \left( \frac{w_0 + w_1}{a} \right)^2 - \left( \frac{w_1}{a} \right)^2 \right] = \frac{2}{3} \left( \frac{w_0}{a} \right)^2 \left[ 1 + 2 \frac{w_1}{w_0} \right] \quad (D2)$$

The stress corresponding to this strain will be

$$\sigma = \frac{E\epsilon}{1-\mu} = \frac{2}{3} \frac{E}{1-\mu} \frac{w_0^2}{a^2} \left[ 1 + 2 \frac{w_1}{w_0} \right] \quad (D3)$$

Substitution of equation (D3) in (D1) and solution for  $w_0$  gives

$$w_0 = \left[ \frac{3(1-\mu)}{8} \frac{pa^4}{Eh} \frac{1}{1 + 2 \frac{w_1}{w_0}} \right]^{1/3} \quad (D4)$$

The corresponding center deflection  $w_{00}$  for an initially flat membrane would be, with  $w_1 = 0$ ,

$$w_{00} = \left[ \frac{3(1-\mu)}{8} \frac{pa^4}{Eh} \right]^{1/3} \quad (D5)$$

and the increase in center deflection due to bowing is

$$\frac{\Delta w_0}{w_{00}} = \frac{w_0 - w_{00}}{w_{00}} = \left(1 + 2 \frac{w_1}{w_0}\right)^{-1/3} - 1 \approx \frac{2}{3} \frac{w_1}{w_0} \quad (D6)$$

Initial bowing into a spherical surface causes a decrease in center deflection inversely proportional to the center deflection due to the load and directly proportional to the initial bowing at the center.

#### APPENDIX E

##### APPROXIMATE RELATION BETWEEN CENTER DEFLECTION AND PRESSURE (FOLLOWING FÖPPL'S PROCEDURE)

Föppl (reference 9, p. 231) derived an approximate relation between center deflection and pressure for a square plate of medium thickness by assuming that the bending of the plate was proportional to that given by Kirchhoff's theory while the extension was proportional to that for a membrane, so that the total pressure  $p$  was the sum of the pressure  $p_b$  resisted by bending and the pressure  $p_t$  carried by membrane action:

$$p = p_b + p_t \quad (E1)$$

Applying this procedure to a circular plate gives for the deflection as a Kirchhoff plate (reference 5, p. 56):

$$\frac{w_0}{h} = \frac{3}{16} \frac{p_b}{E} \left(\frac{a}{h}\right)^4 (1 - \mu^2) \quad (E2)$$

The center deflection for a circular membrane is, according to Hencky (reference 6), for  $\mu = 0.3$ ,

$$\frac{w_0}{h} = 0.662a \sqrt[3]{\frac{p_t a}{E h^4}} \quad (E3)$$

Solving equations (E2) and (E3) for  $p_b$  and  $p_t$ , respectively, and substituting in (E1) leads to the desired relation:

$$\frac{w_0}{h} + 0.588 \left( \frac{w_0}{h} \right)^3 = \frac{3}{16} \frac{p}{E} \left( \frac{a}{h} \right)^4 (1 - \mu^2) \quad (B4)$$

National Bureau of Standards,  
Washington, D. C., October 10, 1941.

#### REFERENCES

1. Way, Stewart: Bending of Circular Plates with Large Deflection. A.S.M.E. Trans., APM-56-12, vol. 56, no. 8, Aug. 1934, pp. 627-636.
2. Hamberg, Walter, McPherson, Albert E., and Levy, Sam: Experimental Study of Deformation and of Effective Width in Axially Loaded Sheet-Stringer Panels. T.N. No. 684, NACA, 1939.
3. Greenspan, Martin: Approximation to a Function of One Variable from a Set of Its Mean Values. Res. Paper 1235, Nat. Bur. Of Standards Jour. Res., vol. 23, no. 2, Aug. 1939, pp. 309-317.
- ✓ 4. Meisse, L. A.: Improvement in the Adaptability of the Tuckerman Strain Gage. A.S.T.M. Proc., vol. 37, pt. II, 1937, pp. 650-654.
5. Nadai, A.: Elastische Platten. Julius Springer (Berlin), 1925.
6. Hencky, H.: Ueber den Spannungszustand in kreisrunden Platten mit verschwindender Biegesteifigkeit. Z. f. Math. u. Phys., vol. 63, 1915, p. 311.
7. Timoshenko, S.: Vibration Problems in Engineering. D. Van Nostrand Co., Inc., 1928.
8. Federhofer, K.: Zur Berechnung der dünnen Kreisplatte mit grosser Ausbiegung. Forschung auf dem Gebiete des Ingenieurwesens Ausg. B, Bd. 7, Heft 3, VDI-Verlag G.m.b.H. (Berlin), May/June 1936, pp. 148-151.
9. Föppl, August, and Föppl, Ludwig: Drang und Zwang. Vol. I, R. Oldenbourg (Munich), 2d ed., 1924.



10. Boobnov, Ivan G.: On the Stresses in a Ship's Bottom Plating Due to Water Pressure. Trans. Inst. Naval Arch., vol. XLIV, 1902, pp. 15-52.
11. Nadai, A.: Plasticity. McGraw-Hill Book Co., Inc., 1940.
12. Timoshenko, S.: Strength of Materials, pts. I and II. D. Van Nostrand Co., Inc., vol. 2, 1930, p. 511.

TABLE I.- SUMMARY OF NORMAL-PRESSURE TESTS OF RIGIDLY CLAMPED CIRCULAR PLATES 5 INCHES IN DIAMETER

Material	Plate	Thickness, h (in.)	Young's modulus (kips/sq in.)	Tensile yield strength		Navy yield pressure (lb/sq in.)	Pressure for given set	
				Longitudinal (kips/sq in.)	Transverse (kips/sq in.)		diameter 500 (lb/sq in.)	diameter 200 (lb/sq in.)
24S-RT Aleled aluminum alloy	A	0.0632	10,400	62.6	52.0	96	107	159
	B	.0504	10,400	59.8	49.5	84	74	120
	C	.0406	10,400	57.2	49.2	42	57	91
17S-RT aluminum alloy	D	.0723	10,300	55.5	46.6	133	149	191
	E	.0658	10,300	51.0	43.8	106	119	157
	F	.0525	10,300	54.4	43.0	76	95	127
	G	.0455	10,300	49.4	45.5	61	76	99
	H	.0387	10,300	51.2	46.6	54	68	88
	I	.0300	10,300	50.1	44.0	38	48	65
	J	.0257	10,300	52.3	46.9	33	38	53
	K	.0211	10,300	53.9	48.2	28	35	50
	L	.0627	10,500	50.2	41.7	81	92	125
17S-T aluminum alloy	M	.0320	10,400	45.5	37.9	23	37	60
	N	.0209	10,500	45.3	37.9	21	35	62
Aluminum alloy	O	.0150	10,500	34.5	31.2	5	7	12
24S-T aluminum alloy	P	.0184	10,500	55.1	48.0	21.5	23.0	25.0
	Q	.0149	10,500	50.8	46.1	22.0	23.5	25.7
18:8 stainless steel	R	.0199	<sup>b</sup> 28,000	177	161.0	33.0	34.0	38.0
24S magnesium alloy	S	.0411	6,400	25.7	25.6	24	24	31

<sup>a</sup>No transverse test was made for specimen N. The value given was arbitrarily taken the same as that for specimen M, which was in the same shipment of material.

<sup>b</sup>Average.

TABLE II.- INDICES FOR DEVIATION FROM IDEAL RIGID CLAMPING

Plate	Thickness, h (in.)	Relative increase in center deflection			Initial deflection per unit thickness, $w_1/h$
		Kirchhoff plate $w_0/h \ll 1$		Membrane $w_0/h \gg 1$	
		Initial tension, equation (1a) $(\Delta w_0/w_{00})_A$	Rotation of edges, equation (2) $(\Delta w_0/w_{00})_B$	Radial contraction of clamping ring, equation (3) $(\Delta w_0/w_{00})_C$	
A	0.0632	0.00	0.0000	0.0066	0.003
B	.0504	-.14	.0000	.0052	-.034
C	.0406	-.13	.0000	.0043	-.020
D	.0723	.13	.0000	.0076	.001
E	.0658	-.01	.0000	.0069	-.003
F	.0525	-.03	.0000	.0055	-.006
G	.0453	-.02	.0000	.0048	-.009
H	.0387	-.27	.0000	.0041	-.049
I	.0300	-.04	.0000	.0031	.043
J	.0257	-.18	.0000	.0027	-.004
K	.0211	-.08	.0000	.0022	.109
L	.0627	.00	.0000	.0066	-.001
M	.0320	.20	.0000	.0034	-.450
N	.0209	.00	.0000	.0022	-.079
O	.0150	.50	.0000	.0015	-.500
P	.0184	-.27	.0000	.0019	-.141
Q	.0149	-.32	.0000	.0016	.038
R	.0199	-.48	.0000	.0057	.136
S	.0411	.01	.0000	.0026	.083

<sup>a</sup>From comparison with Way at low pressures.

Figure 1.-Tensile stress-strain curves  
24SRT alclad aluminum alloy  
used in plates A, B, and C.

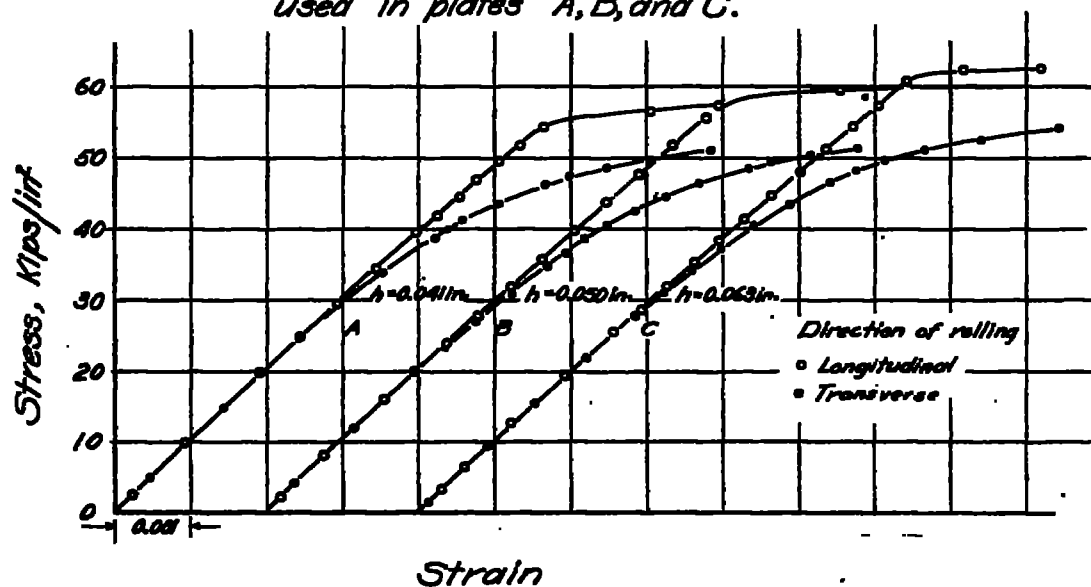


Figure 2.-Tensile stress-strain curves  
17SRT aluminum alloy  
used in plates D, G, H, and K.

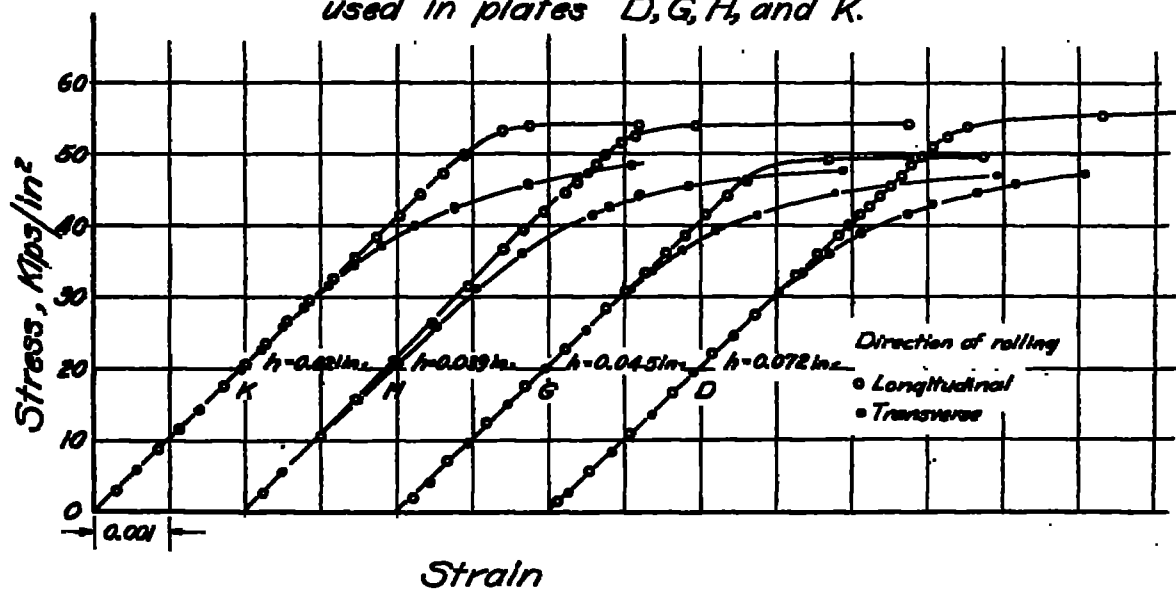


Figure 3.-Tensile stress-strain curves  
179RT aluminum alloy  
used in plates E, F, I, and J.

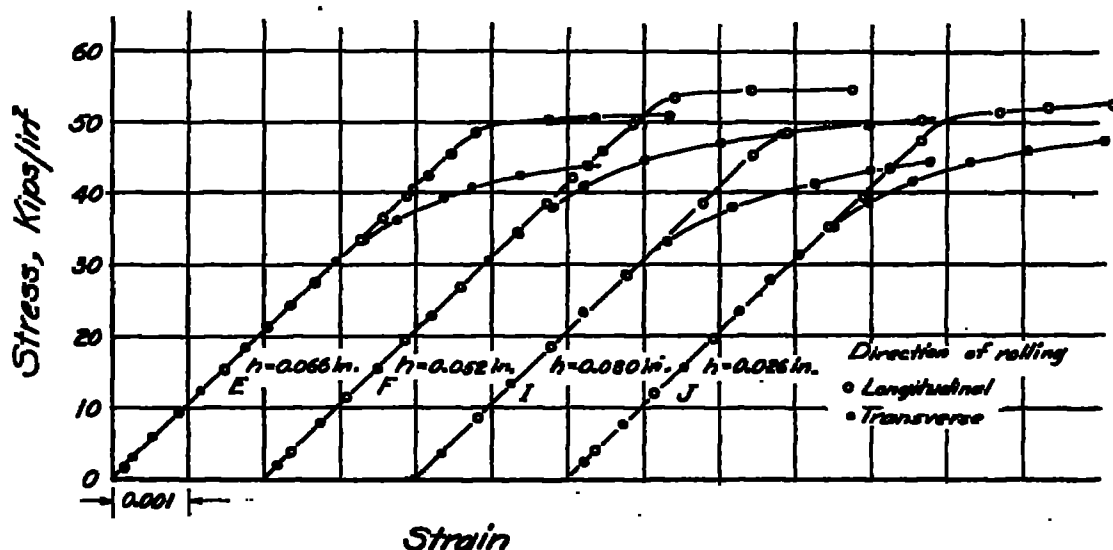


Figure 4.-Tensile stress-strain curves  
175T aluminum alloy  
used in plates L, M, N, and  
Low strength aluminum alloy  
used in plate O.

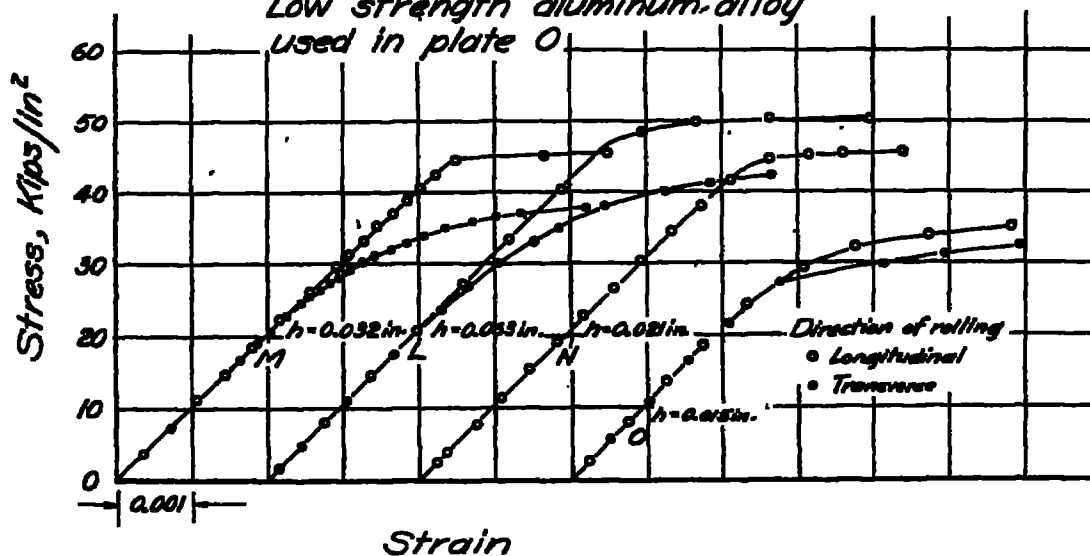


Figure 5-Tensile stress-strain curves  
245T aluminum alloy  
used in plates P and Q

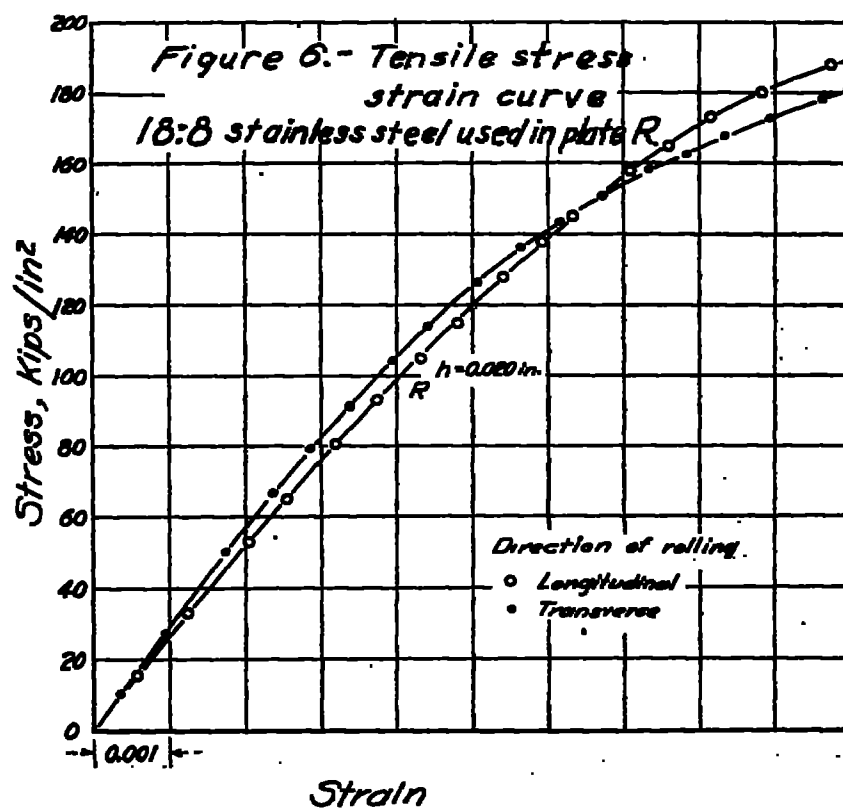
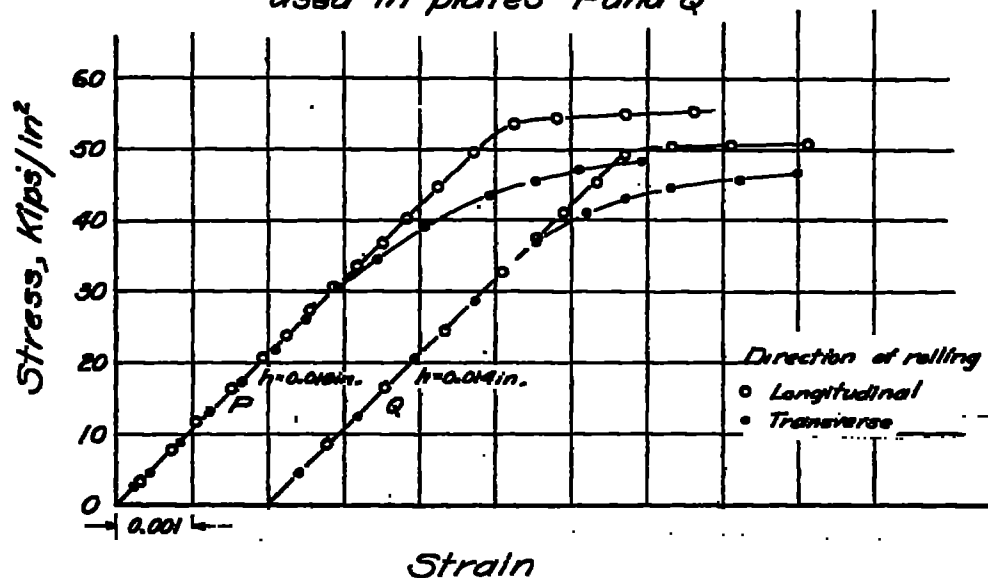


Figure 7.-Tensile stress-strain curve of  
EH magnesium alloy  
used in plate S

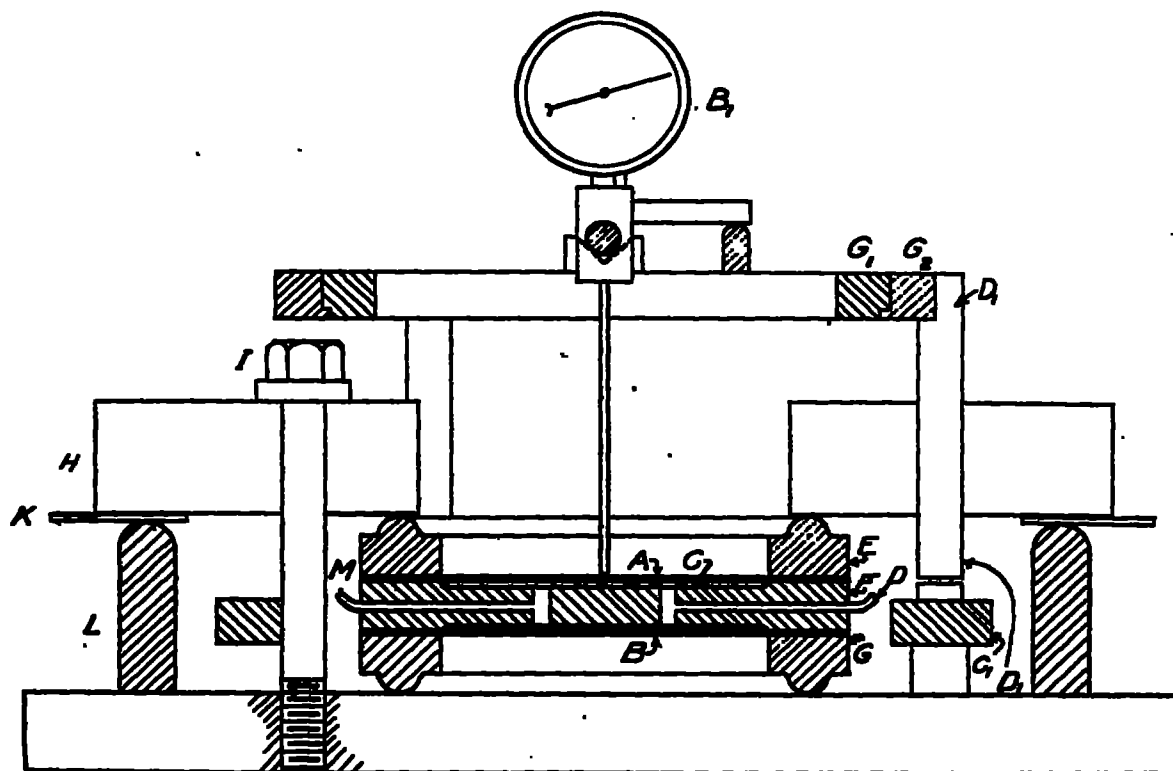
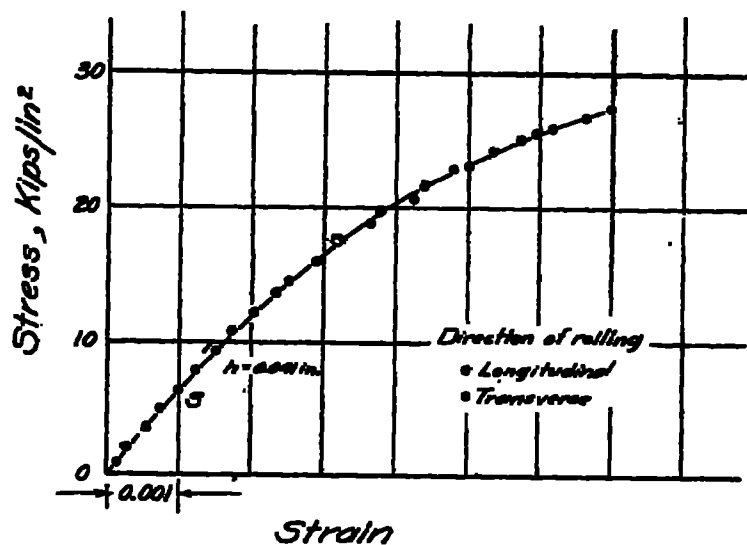


Figure 8.-Vertical section of fixture

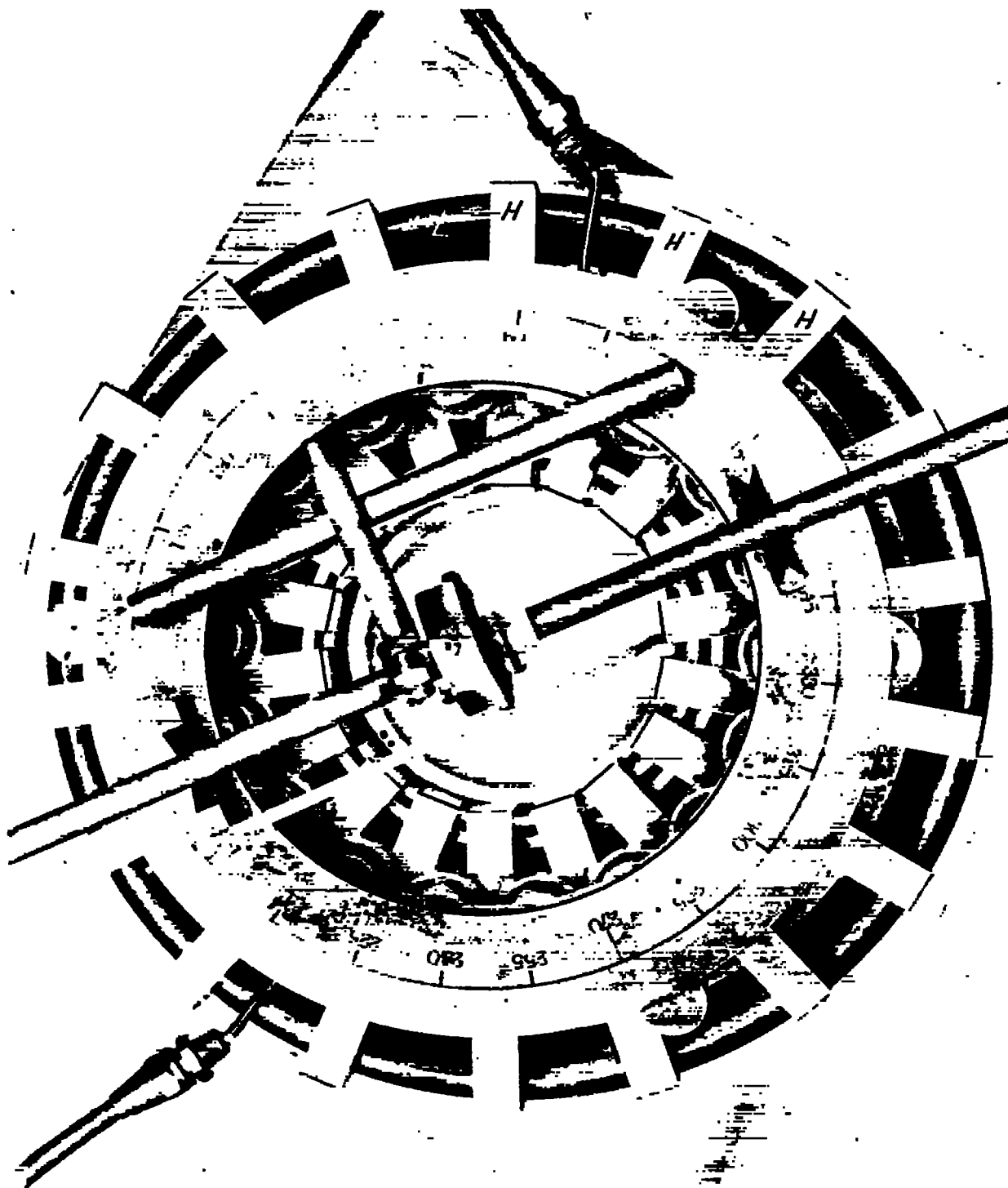


Figure 9.- Top view of plate fixture.



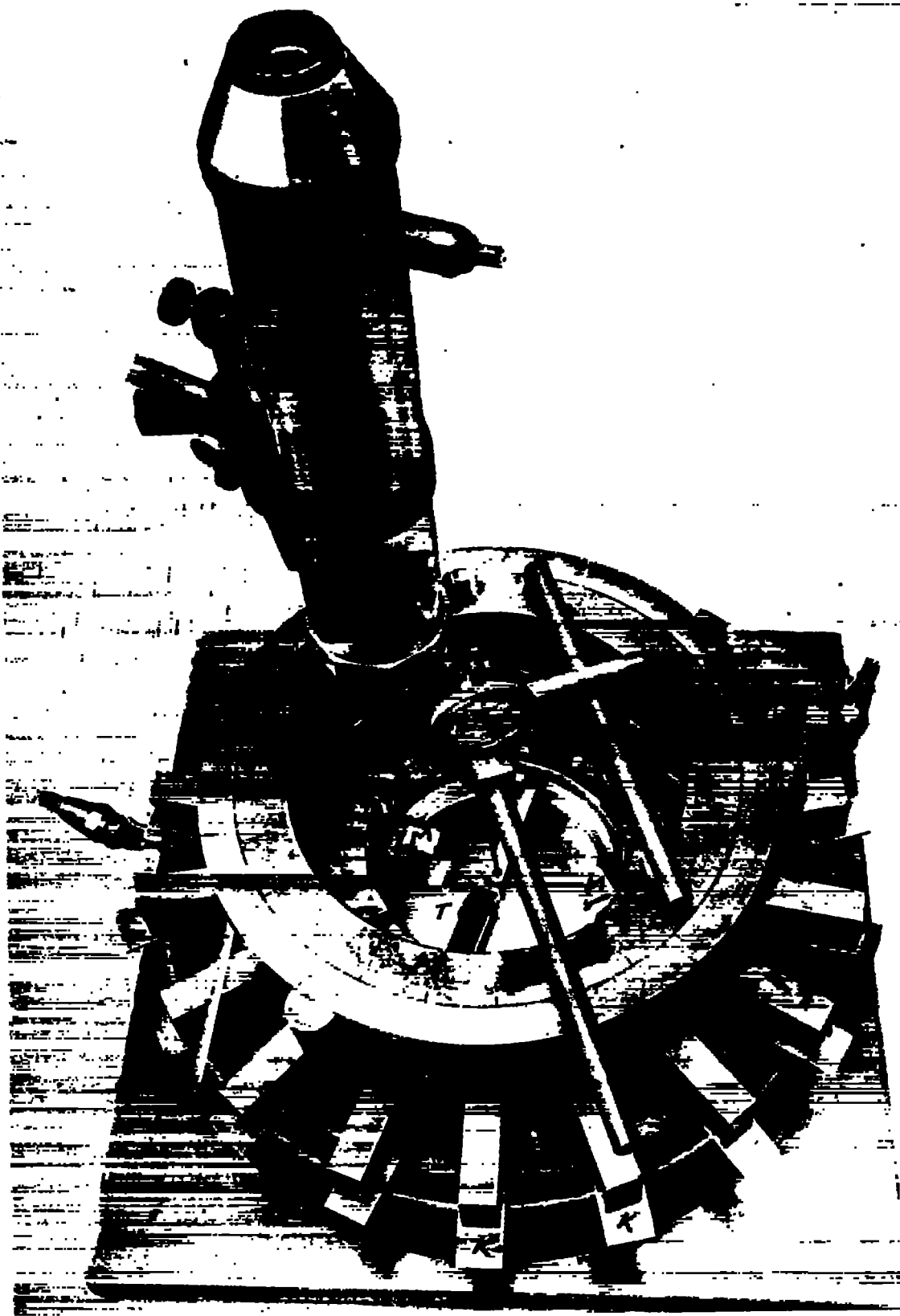


Figure 10.- Measurement of elastic constants of plate fixture.



Figure 11.- Plate fixture, pump, and pressure gages.

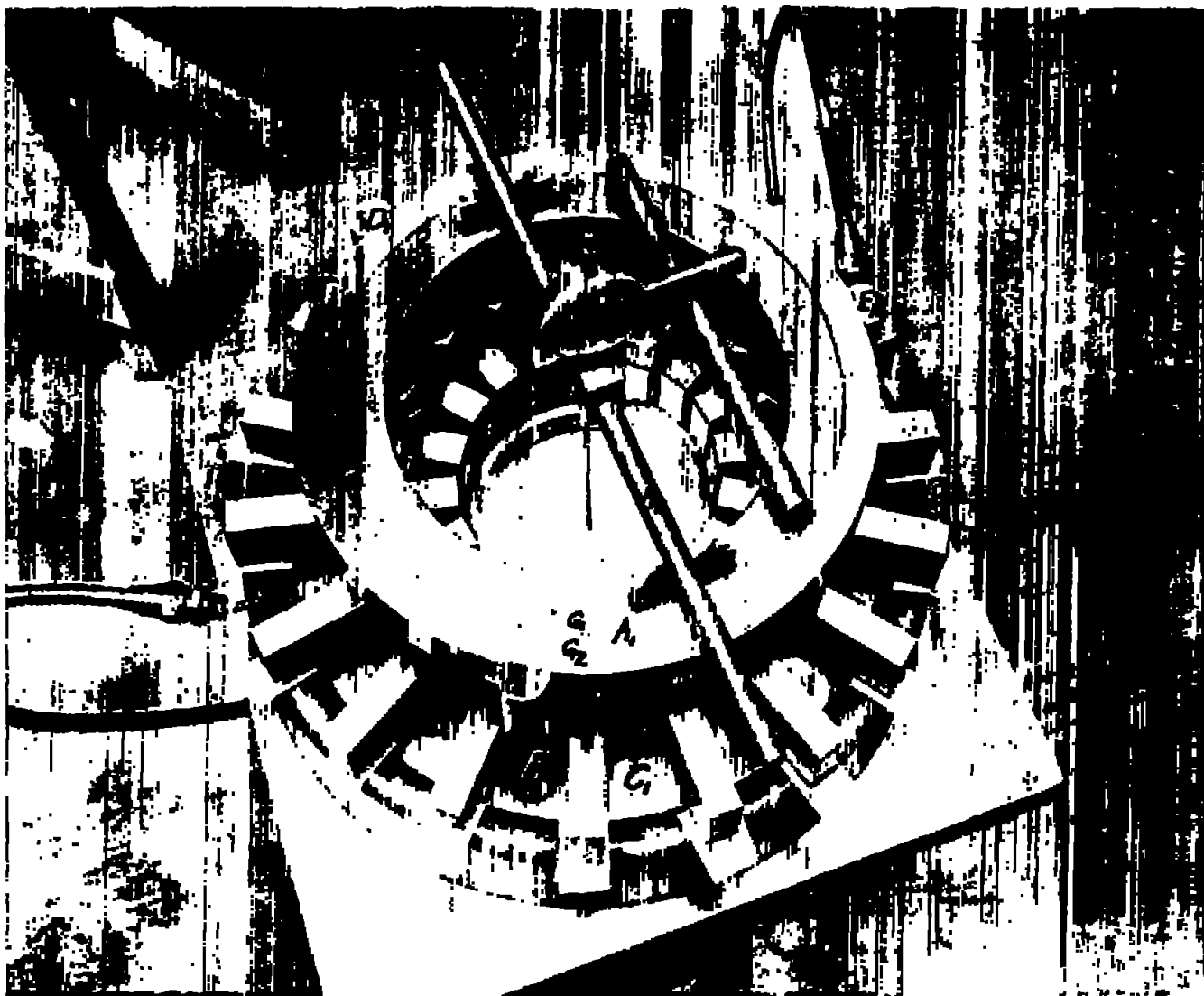


Figure 12.- Measurement of deflection of plate.

Figure 13.- Change in shape of deflection curve with pressure in the elastic range

Test of plate M,  $h=0.032$  in

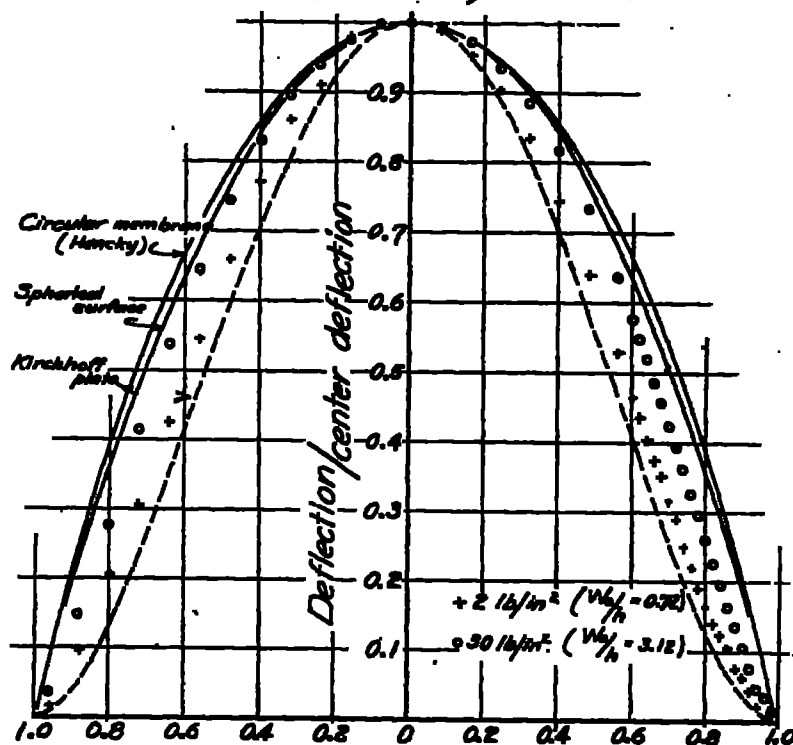


Figure 14.- Normal pressure tests of 24 ST alclad aluminum alloy plates A, B, C

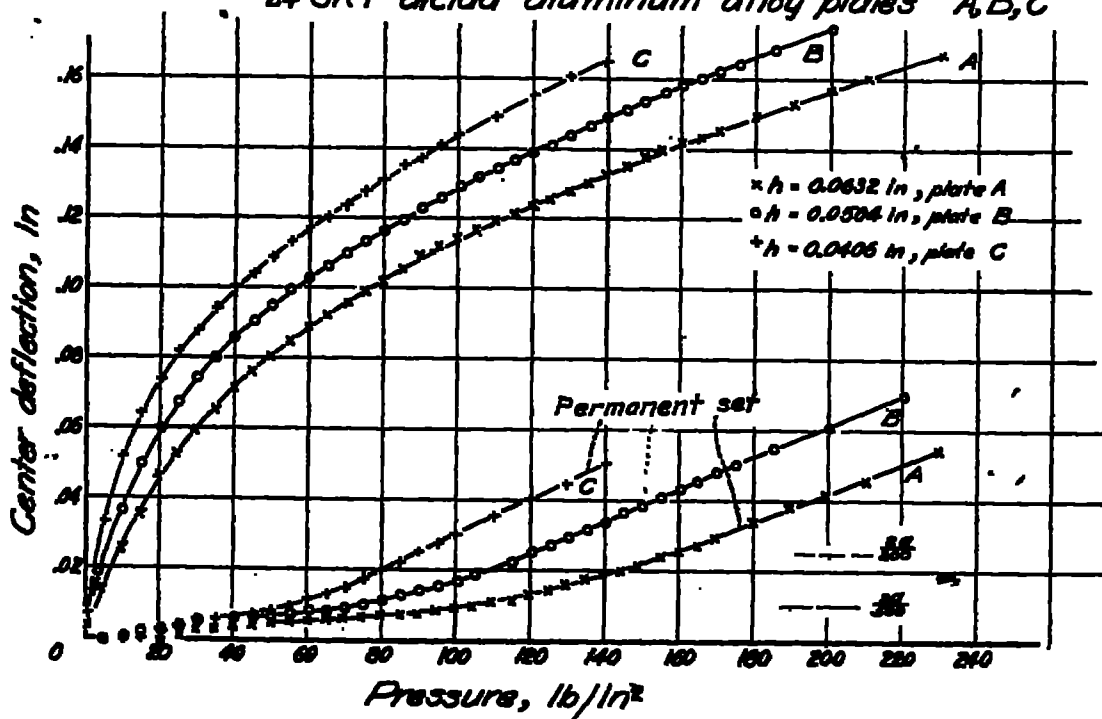


Figure 15.-Normal pressure tests of  
17SRT aluminum alloy plates D,E,F,G,H,I,J,K

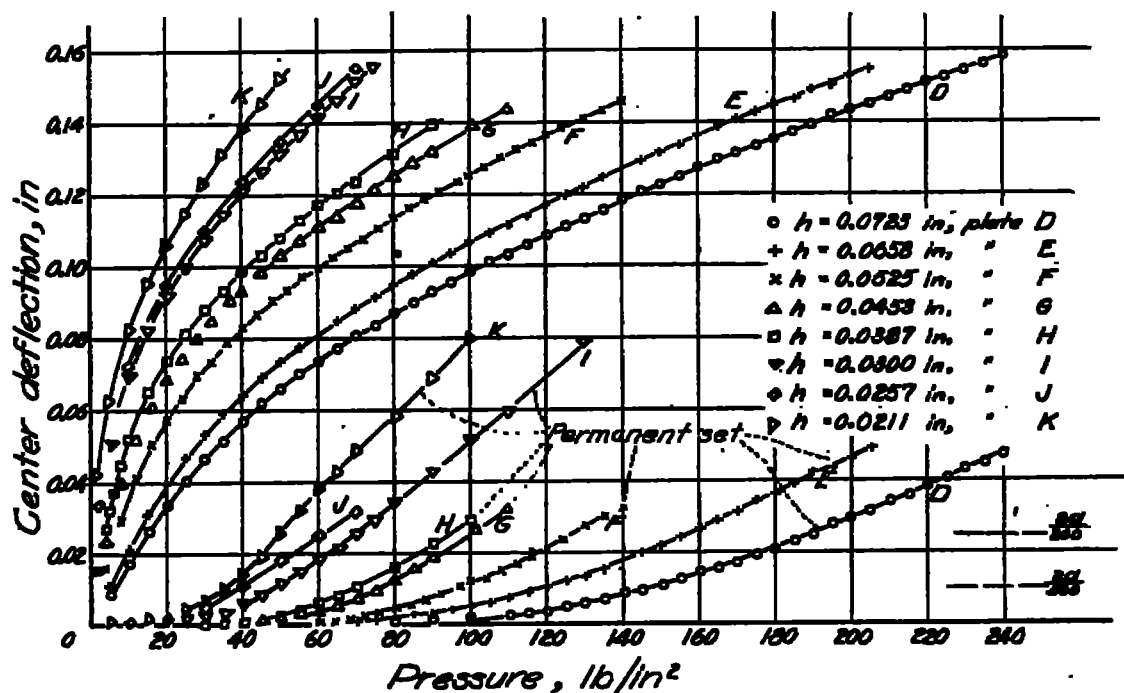


Figure 16.-Normal pressure tests of  
17ST aluminum alloy plates L,M

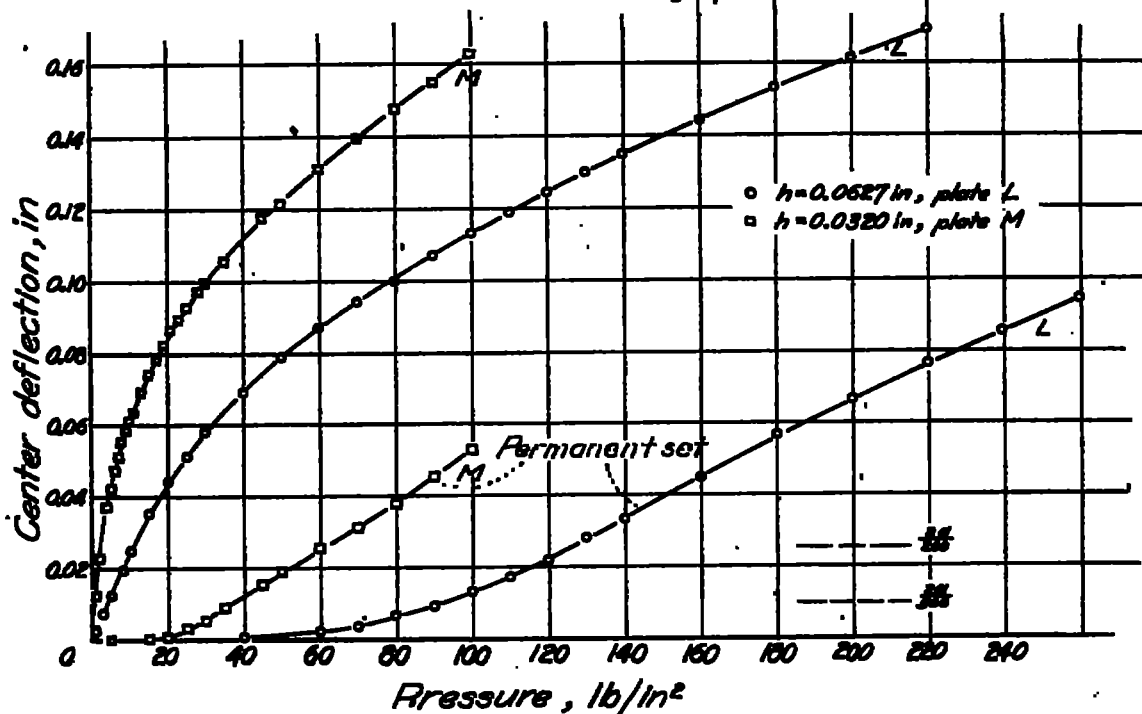


Figure 17.- Normal pressure test of  
175T aluminum alloy plate N and  
low strength aluminum alloy plate O

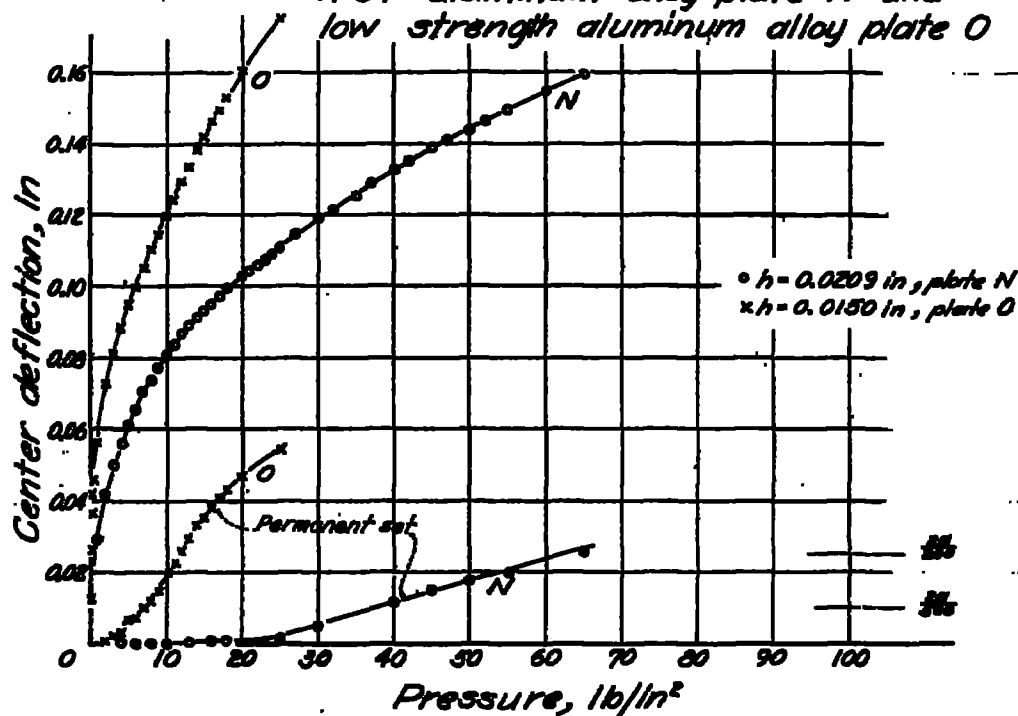


Figure 18.- Normal pressure tests of 245T aluminum alloy  
plates P, Q.

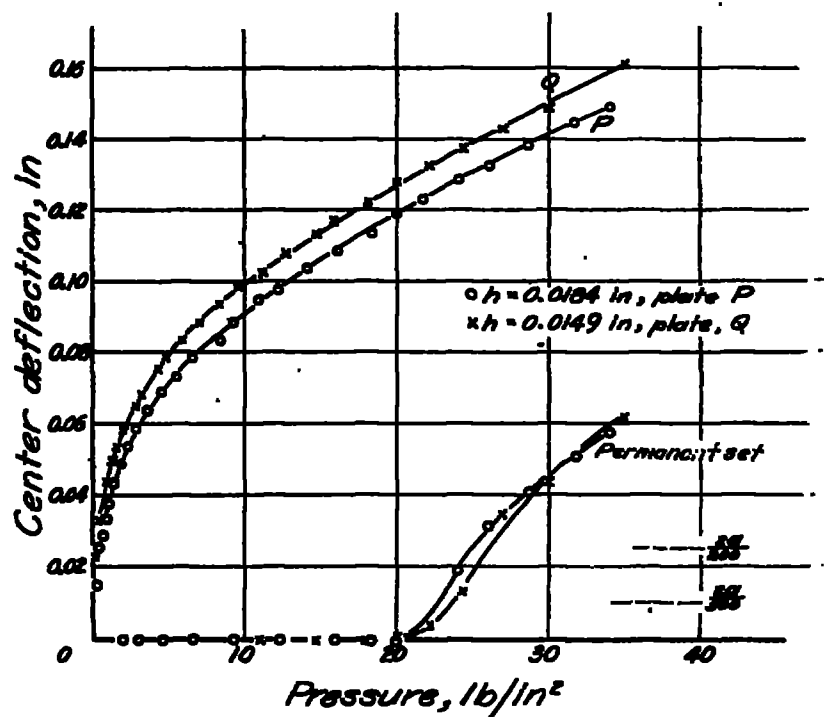


Figure 19.-Normal pressure test of  
18:8 stainless steel plate R

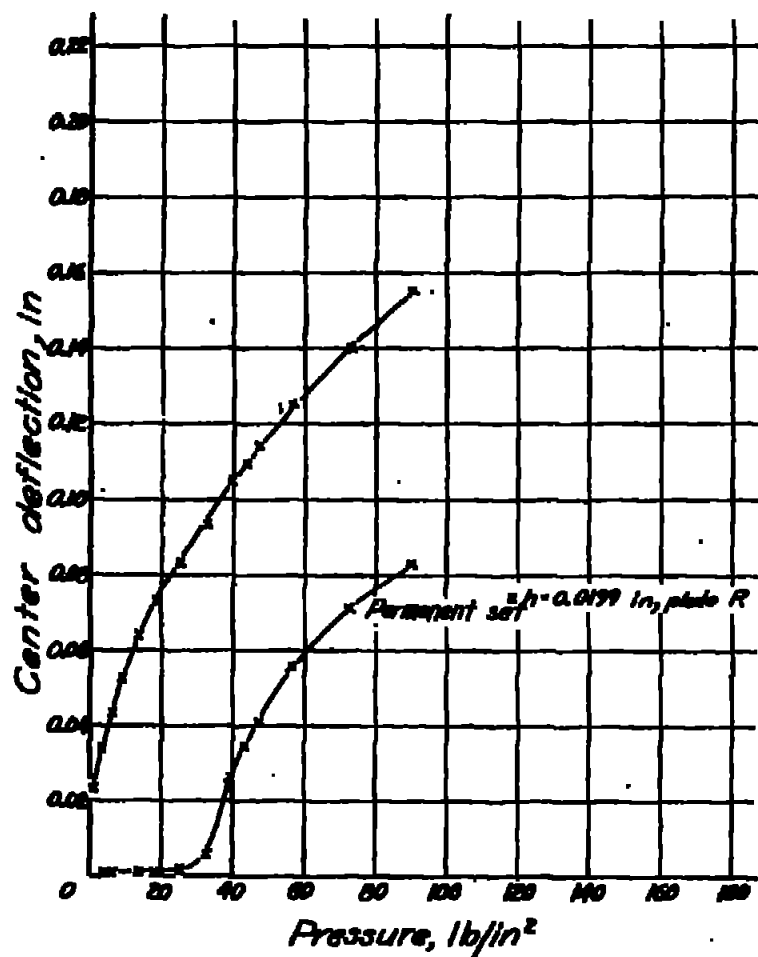
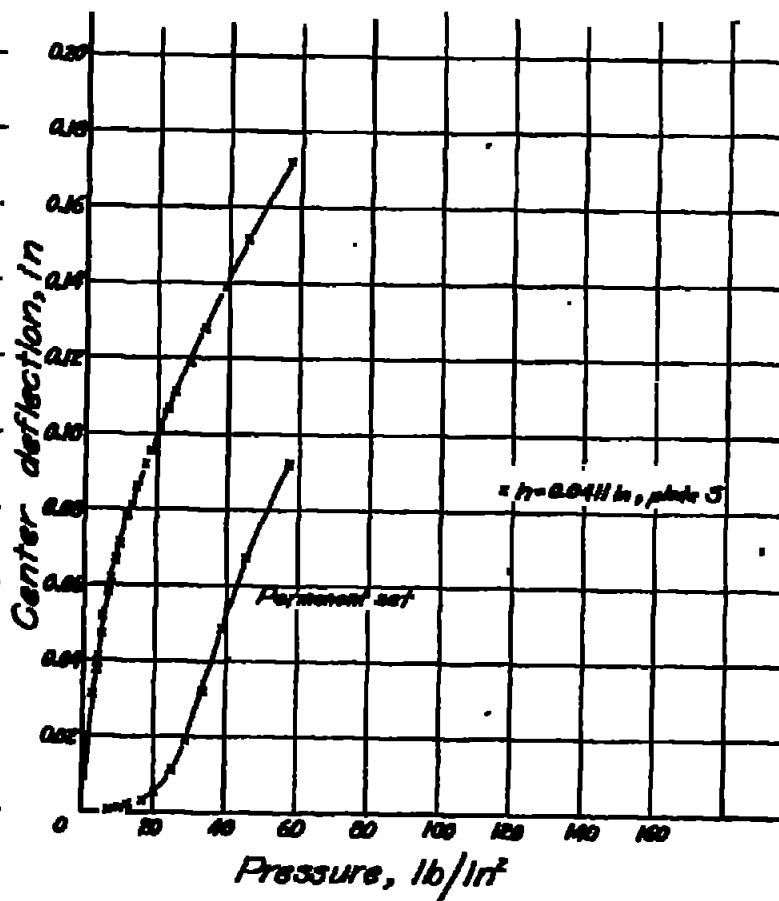


Figure 20.-Normal pressure test of EH  
magnesium alloy plate S



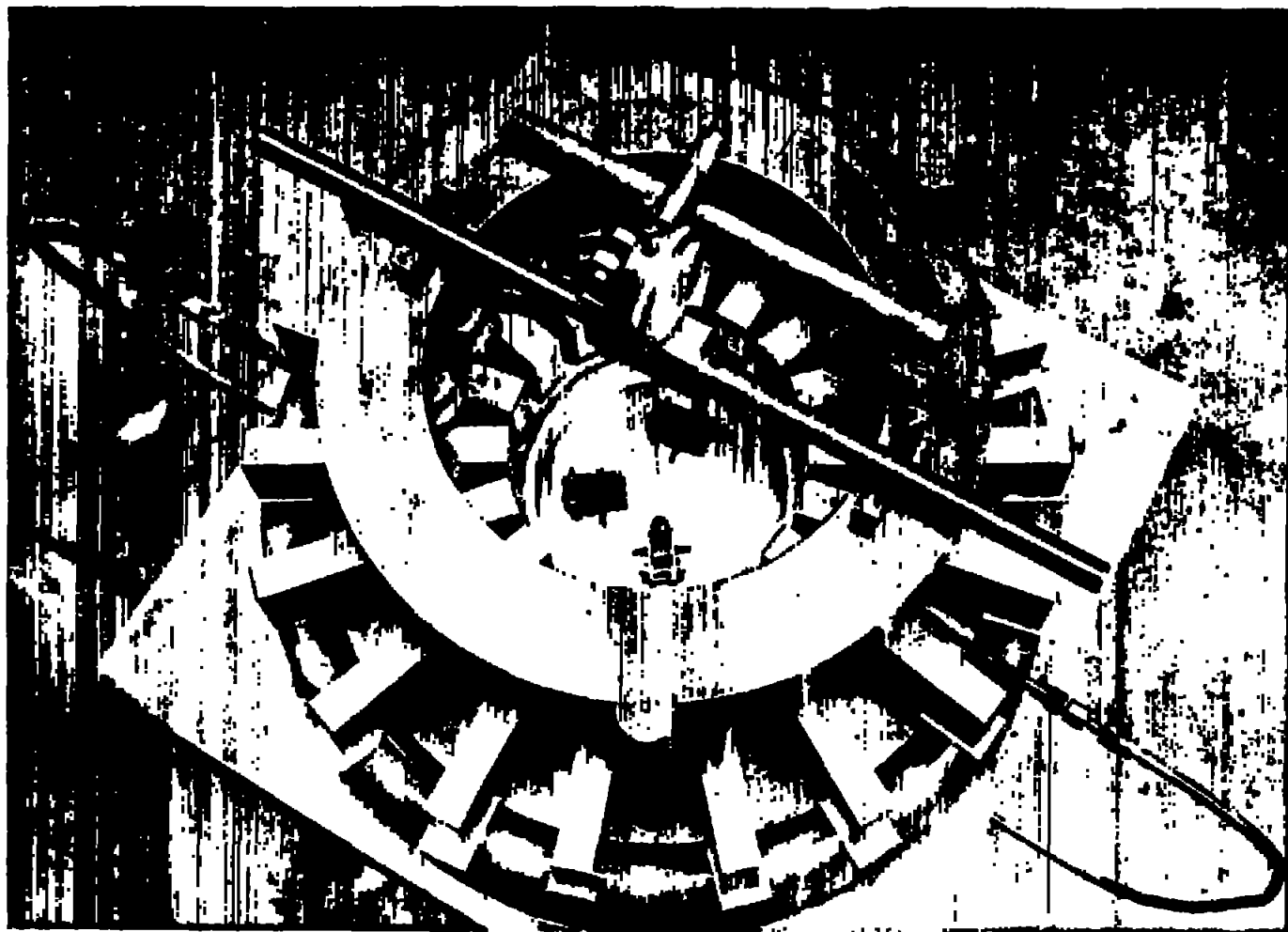


Fig. 21

Figure 21.- Strain measurements on plate M.



Figure 22—Observed strain on plate M  
under normal pressure,  
average over a 1 in gage length

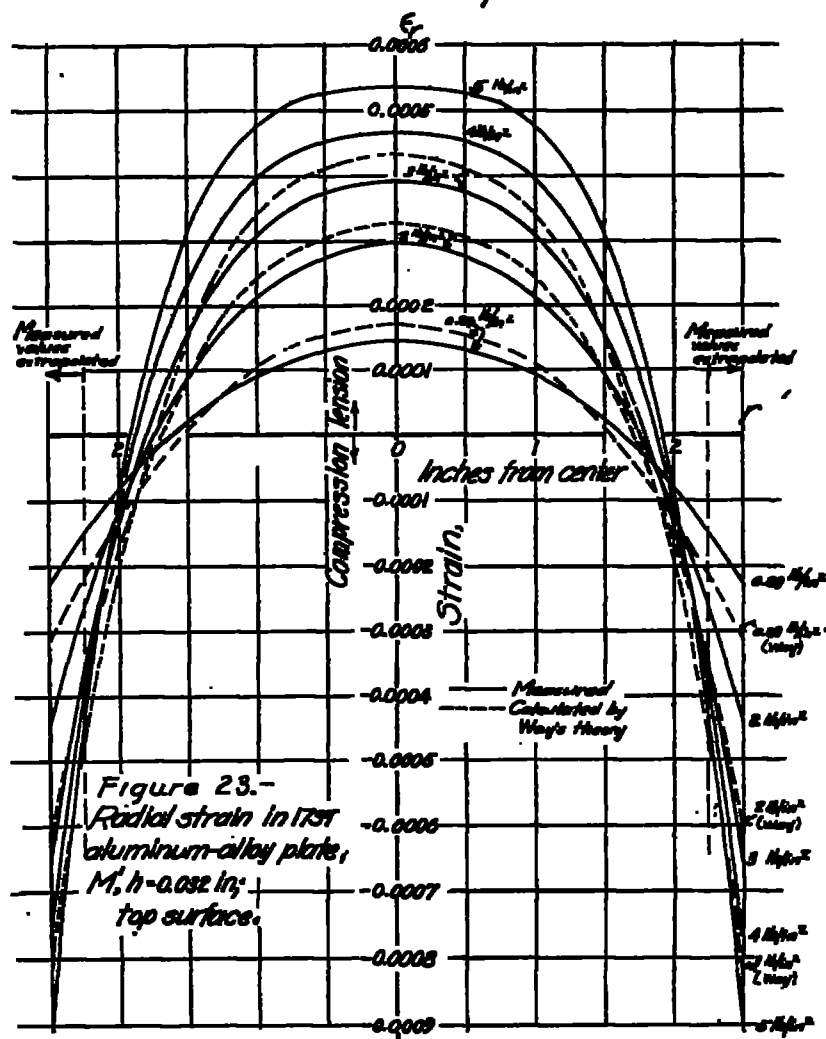
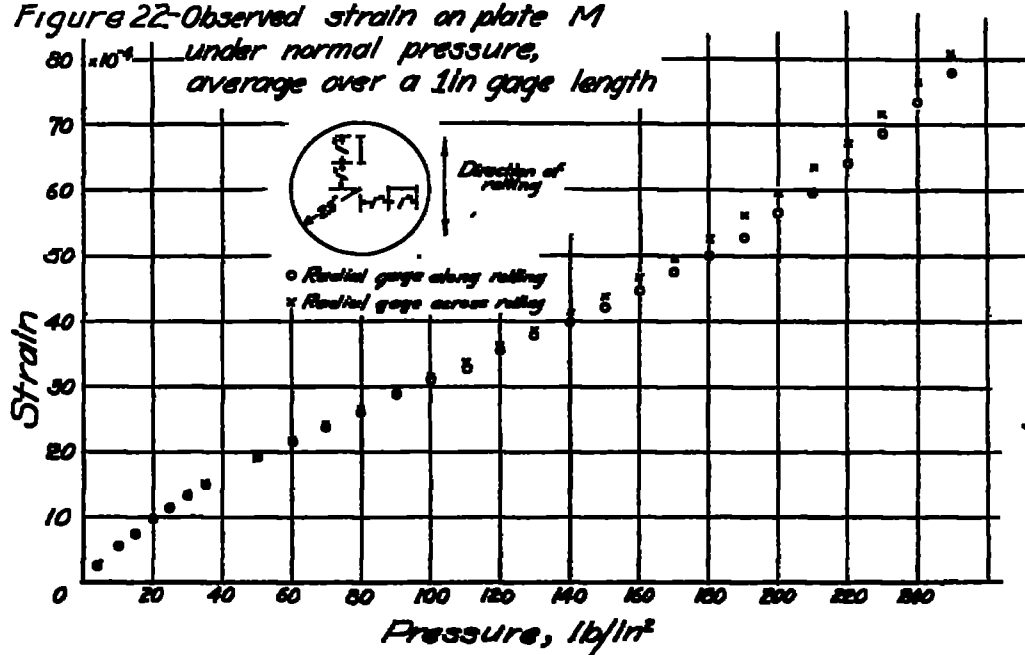


Figure 24.- Radial strain near center  
on  $\frac{1}{10}$ -in. gage length  
175T aluminum-alloy plate M<sup>a</sup>  
 $h=0.052$  in

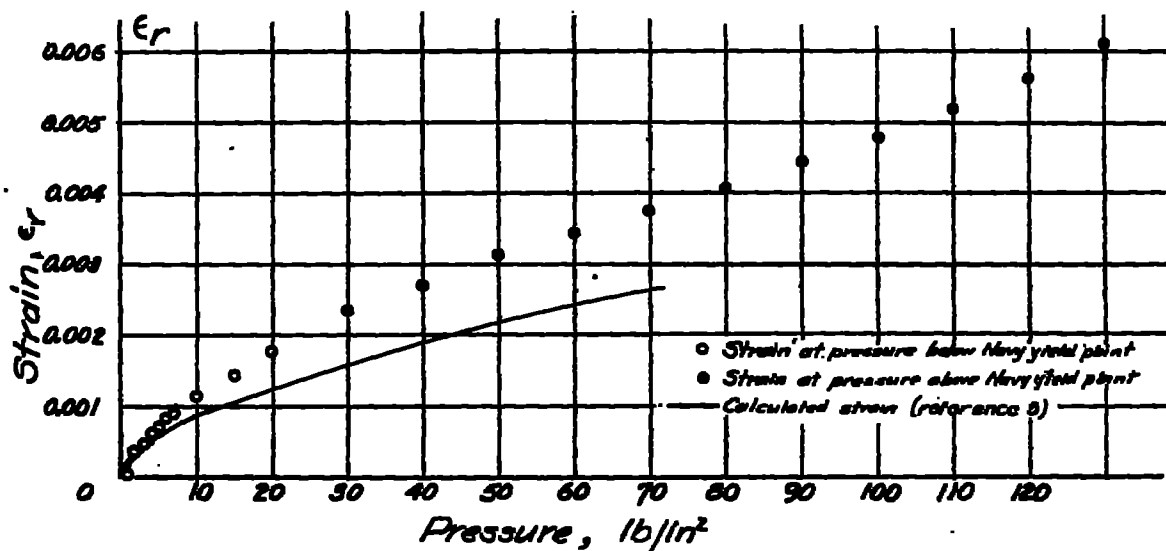


Figure 25.- Shape of deflection curve with large amount of yielding

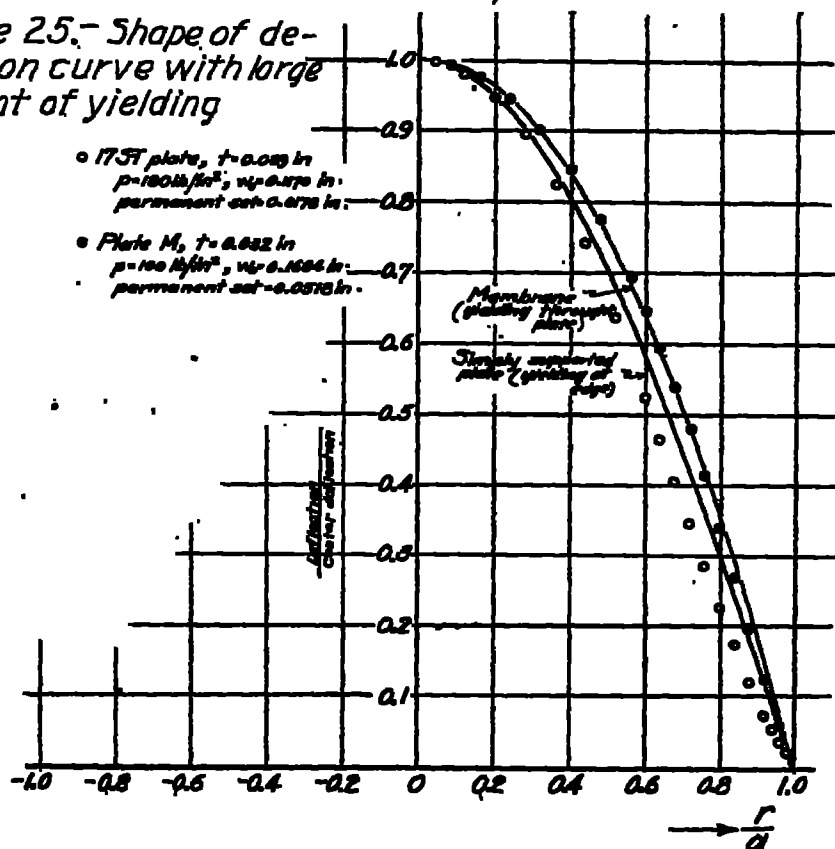


Figure 26.- Elastic center deflection  
vs. pressure curves

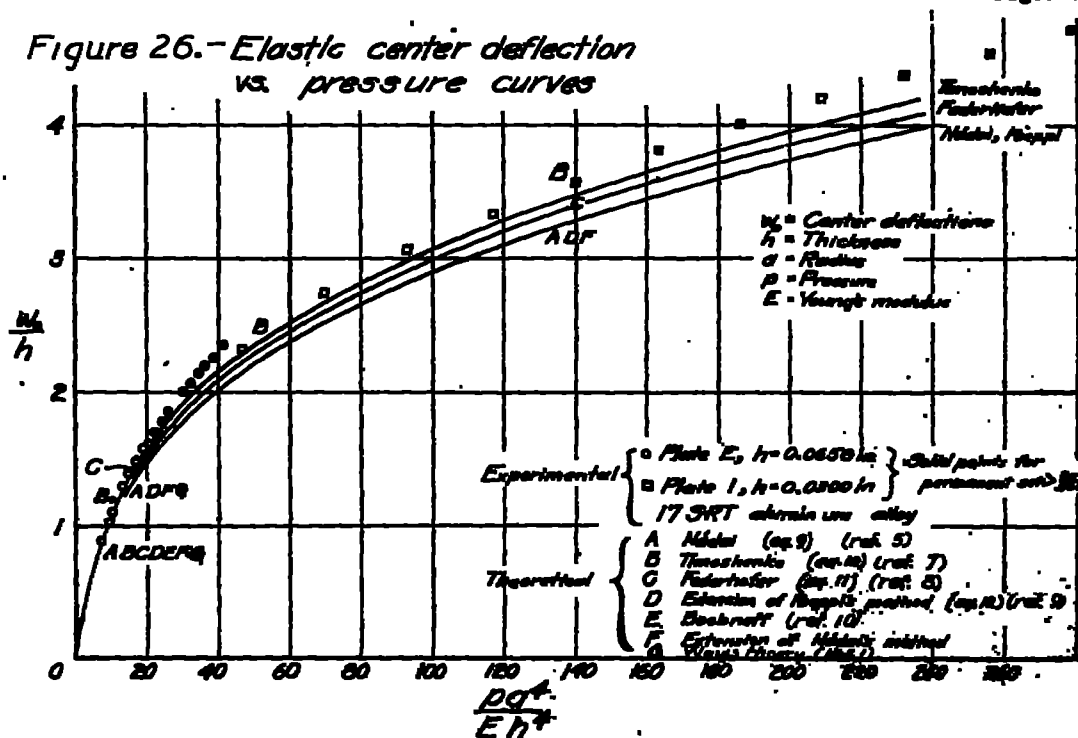
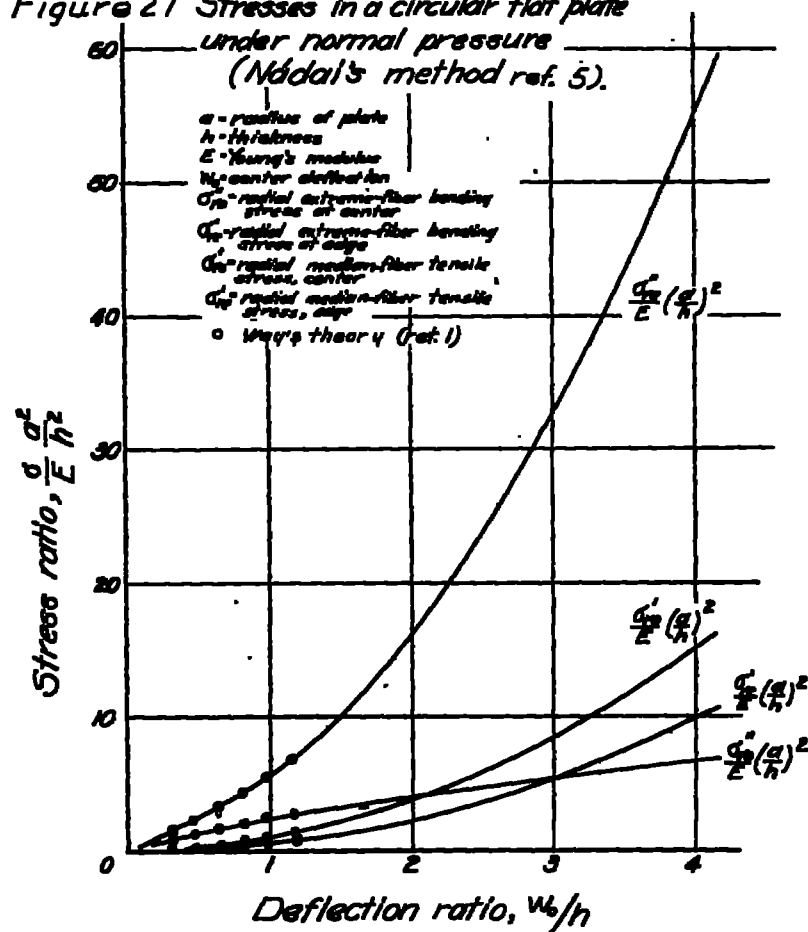


Figure 27 Stresses in a circular flat plate  
under normal pressure  
(Miki's method ref. 5).



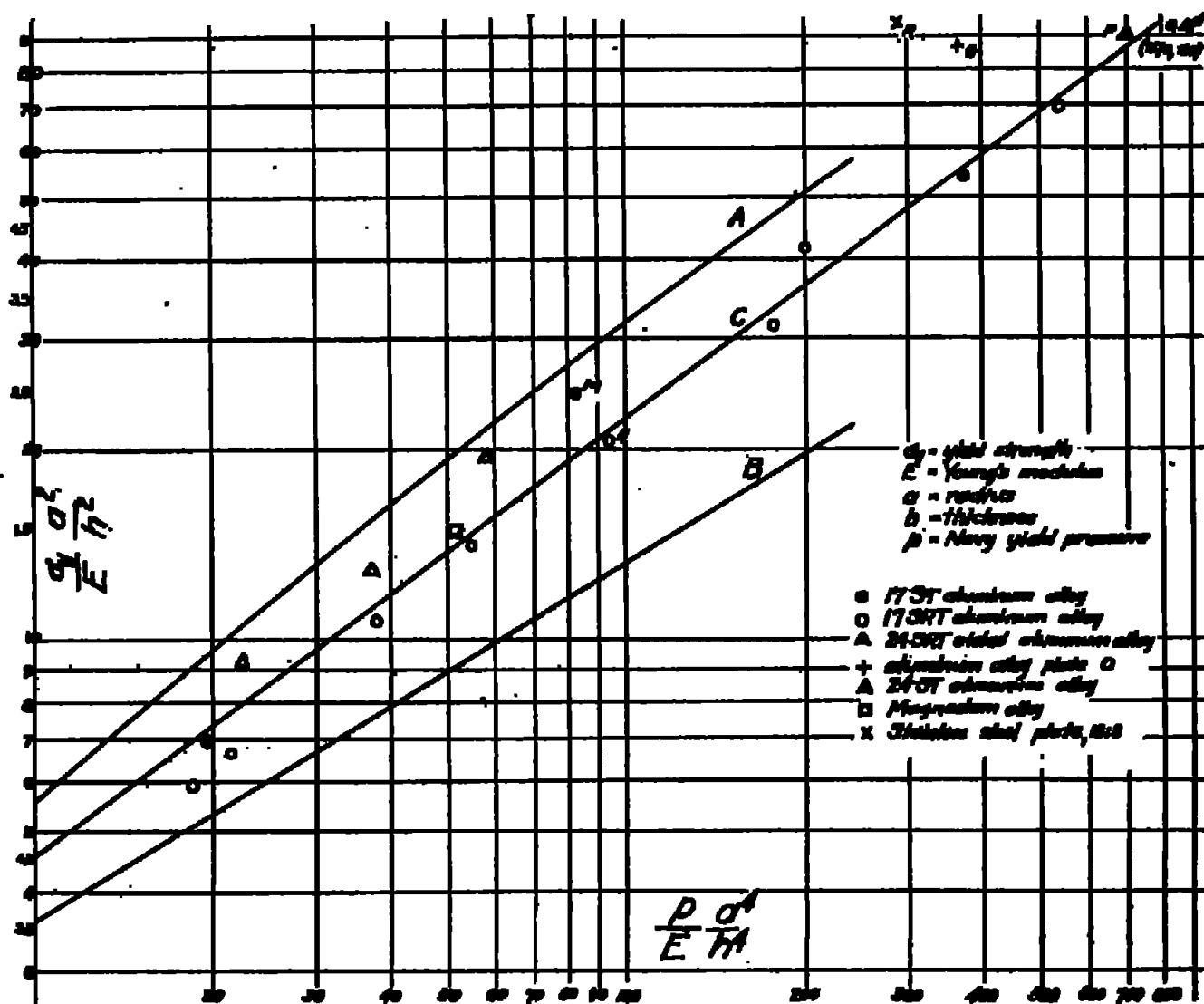


Figure 2A- Relation between  $\frac{\sigma_y}{E}$  and  $\frac{P}{\sigma_y}$  for Navy yield pressure

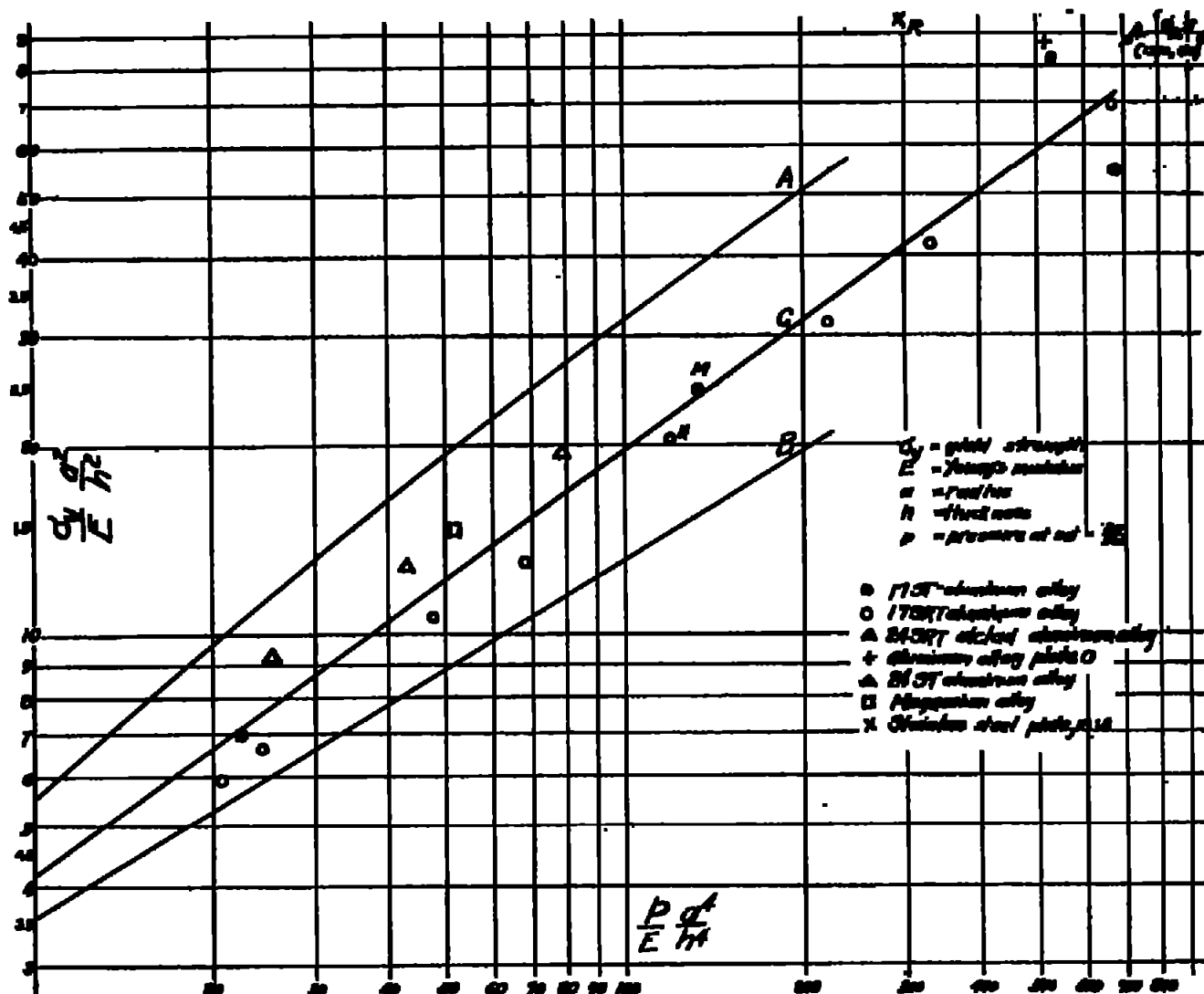


Figure 29- Relation between  $\frac{\sigma_y}{E}$  and  $\frac{p}{E}$  for pressure at set 2a/500.

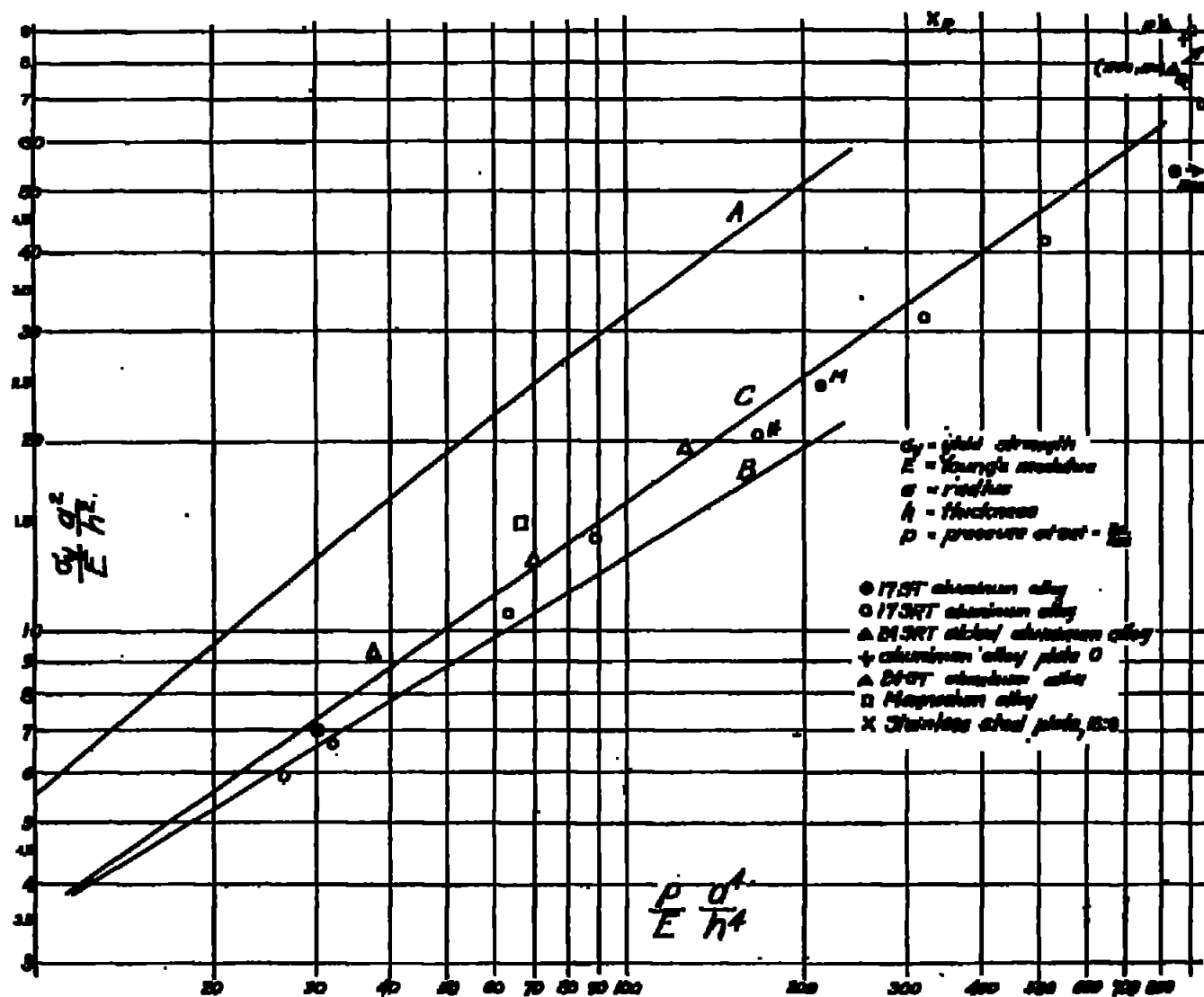


Figure 30.- Relation between  $\frac{\sigma_y}{E_s} \frac{d^2}{h^2}$  and  $\frac{p}{E_s} \frac{d^4}{h^4}$  for pressure at set 2a/200.

Figure 31.- Center deflection at Navy yield pressure

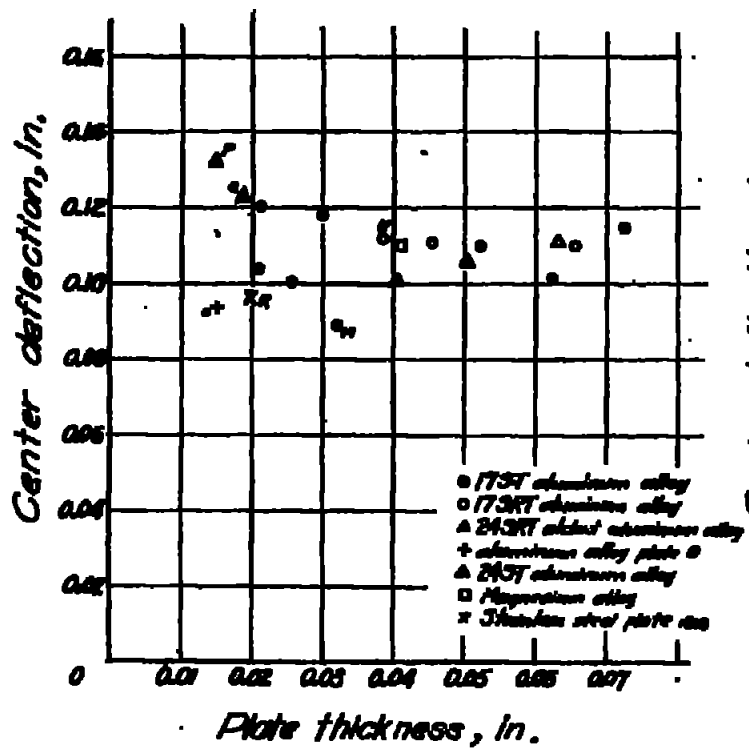


Figure 32 Center deflection. when set at center -  $\frac{29}{350}$

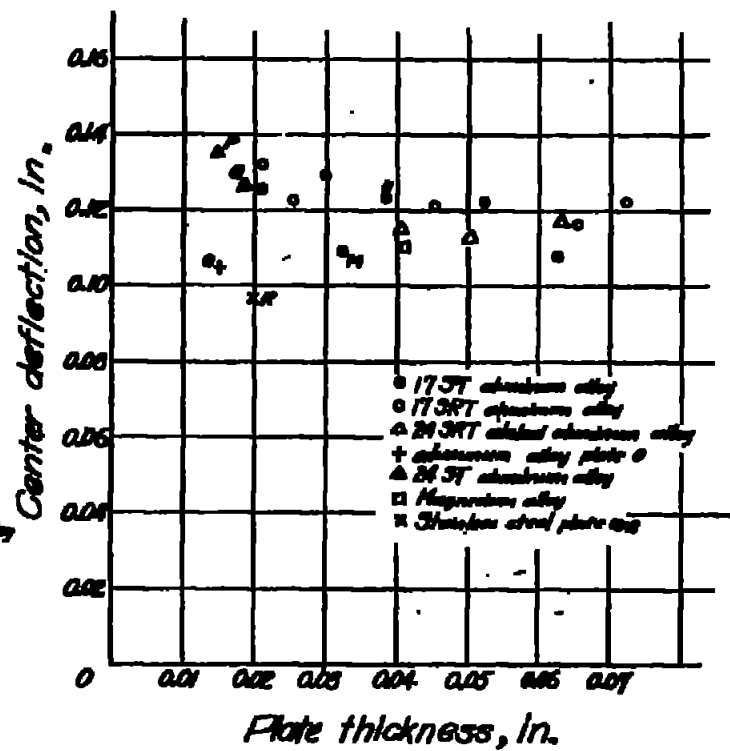


Figure 33. Center deflection when  
set at center -  $\frac{\delta l}{l_0}$

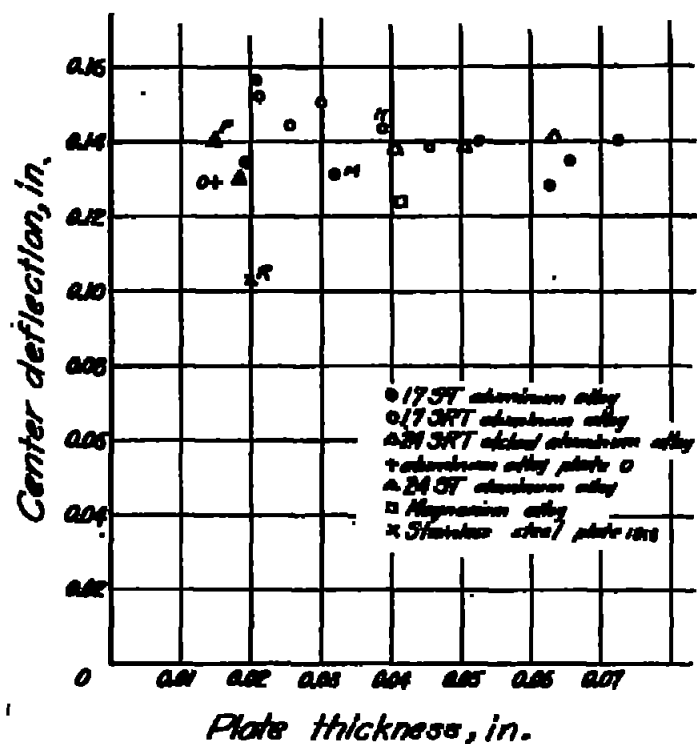


Figure 34. Navy yield pressure

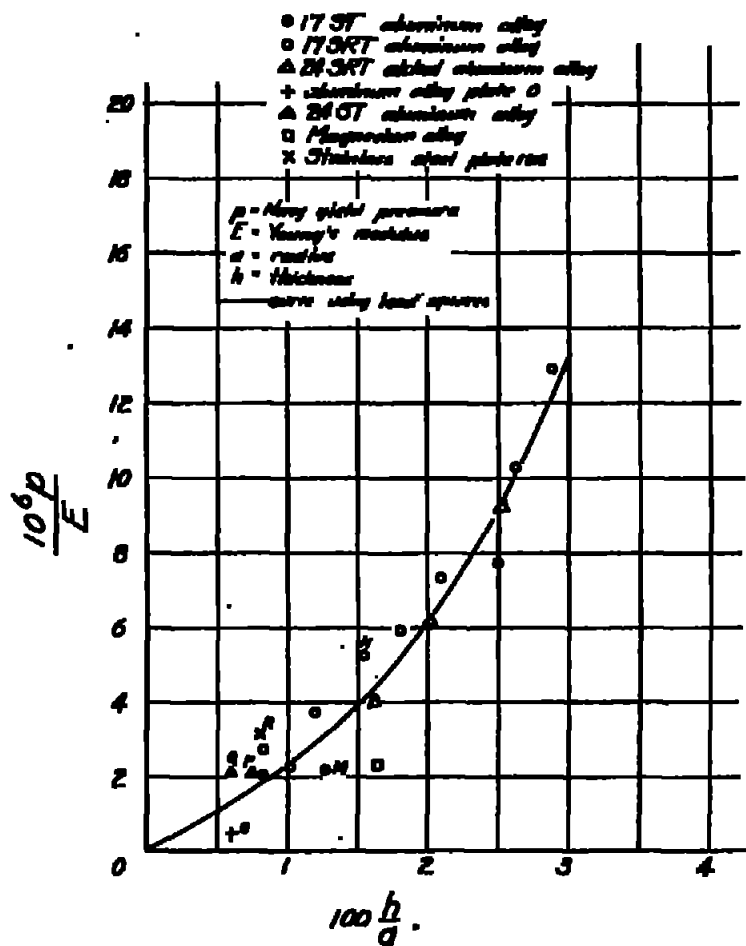




Figure 35-Pressure for permanent set  
at center -  $\frac{2a}{3b}$

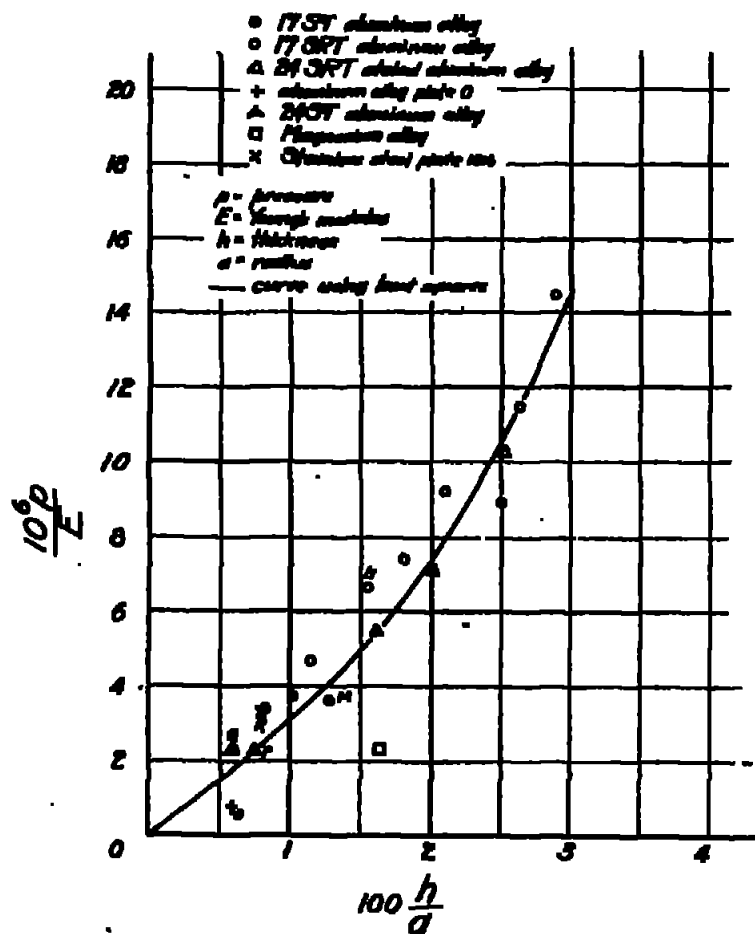


Figure 36-Pressure for permanent set  
at center -  $\frac{2a}{3b}$

